JOC The Journal of Organic Chemistry

Article

pubs.acs.org/joc

Nonstatistical Dynamic Effects in the Thermal C^2–C^6 Diels–Alder Cyclization of Enyne–Allenes

Debabrata Samanta, Mehmet Emin Cinar, Kalpataru Das, and Michael Schmittel*

Department of Chemistry and Biology, Universität Siegen, Adolf-Reichwein-Strasse, D-57068 Siegen, Germany

Supporting Information

ABSTRACT: The Diels–Alder (DA) reaction channel of the thermal C^2–C^6 (Schmittel) cyclization of enyne–allenes is studied computationally and experimentally evaluating the influence of temperature on product ratios. Remote substituents at the alkyne terminus influence the mechanism of the C^2–C^6/DA cyclization steering it either to a stepwise or a concerted course. Temperature independent product ratios, selectivity of product formation, and computational results obtained at (U)BLYP/6-31G(d) level unveil a mechanism that is strongly controlled by nonstatistical dynamics.

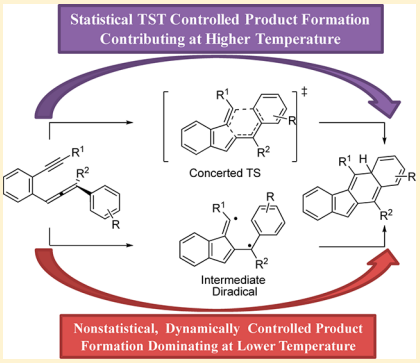

INTRODUCTION

The elucidation of a reaction mechanism is one of the classical tasks and challenges in physical organic chemistry. Traditionally, our conceptual approach to understand kinetically controlled reaction schemes is based on well-founded textbook knowledge of kinetics and guided either by transition state theory (TST)[1] applying a classical statistical ansatz or by the RRKM (Rice–Ramsperger–Kassel–Marcus) theory.[2] According to the latter, which is a microcanonical theory, the energy obtained from collisions of molecules has to be concentrated in proper vibrational modes to cross the activation barrier. In a multistep process, the various intermediates will thus have initially those vibrations populated that had been selected by the preceding transition-state passage. If intramolecular vibrational energy redistribution (IVR) of kinetic energy takes place in the ensuing intermediate prior to undergoing the follow-up reaction, then the intermediate will obey statistical kinetics. However, if the follow-up reaction is faster than IVR, then the intermediate will show non-RRKM behavior that is denoted as nonstatistical dynamics. There is a wide variety of systems reacting via S_N2 ion–dipole complexes,[3] organic diradicals,[4] radical cations,[5] radicals,[5c,6] and carbocations[7] that cannot be explained on the basis of classical TST. Particularly at the boundary of highly asynchronous concerted and stepwise mechanisms, processes have been demonstrated to be subject to nonstatistical dynamic effects.[3c,8,9]

Thermal cycloaromatizations of enediynes (Bergman reaction)[10] and of enyne–allenes (Myers–Saito/C^2–C^7 cyclization)[11] have received ample attention over the last two decades[12,13] as the resultant diradicals represent key intermediates in the mode of action of natural enediyne antitumor antibiotics.[14] In 1995, Schmittel et al. disclosed a competing thermal reaction mode to the well-known Myers–Saito cyclization, denoted as the C^2–C^6 or Schmittel cyclization of enyne–allenes.[15,16] It has been extensively studied[16] both mechanistically[17] and theoretically[18] due to its value to afford complex carbocycles[19] and to effect DNA cleavage.[20] σ,π-Diradical intermediate **2** (Scheme 1) was successfully trapped with 1,4-cyclohexadiene[17a] and ultrafast radical clocks (diphenylcyclopropyl clock),[21] and computational results as well as the aforementioned observation of DNA double-strand cleavage[20] furnish strong evidence for the cyclization to evolve via a diradical intermediate. The postulated diradical may undergo intramolecular follow-up reactions to furnish the formal Diels–Alder (DA) product **3**,[17b,20a,22] ene product **4**,[15] or [2 + 2] cycloadduct **5**[23] depending on the nature of substituents at the allene terminus (Scheme 1).

Substituents at the alkyne and allene termini may additionally influence the mechanism of the C^2–C^6 cyclization with regard to a stepwise vs concerted course. Experimental studies[24,25] based on radical clock opening and intramolecular kinetic isotope effects (KIEs) as well as theoretical calculations[26] at the (U)B3LYP/6-31G(d) level suggest that the C^2–C^6/ene cyclization proceeds via a diradical mechanism when a radical-stabilizing group such as an aryl unit is located at either the alkyne or allene terminus (Scheme 2).

Singleton and Lipton[27] argue, based on experimental intermolecular KIEs as well as theoretical and dynamic trajectory calculations, that both the stepwise and concerted ene reactions proceed via a single TS and that dynamic effects at a post-transition-state valley–ridge inflection point[28] decide about concerted against stepwise trajectories. The occurrence of dynamic effects has received further experimental backup by

Received: November 19, 2012
Published: February 5, 2013

dx.doi.org/10.1021/jo302524a | J. Org. Chem. 2013, 78, 1451–1462

Scheme 1. Formal Diels–Alder (3), Ene (4), and [2 + 2] Cycloaddition (5) Products from Diradical Intermediate 2

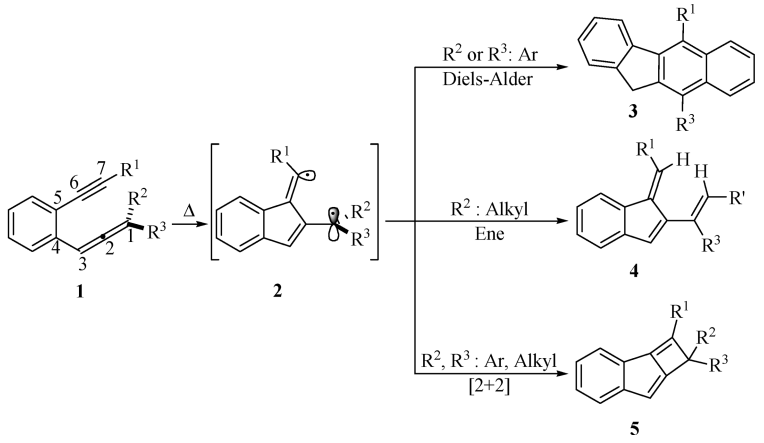

Scheme 2. Mechanistic Options for the Thermal C^2–C^6/Ene Cyclization of Enyne–Allenes[24]

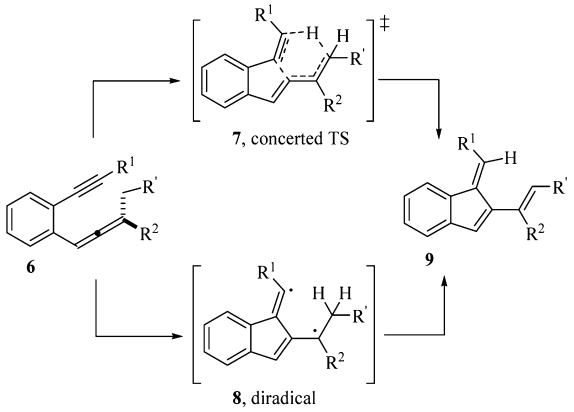

our inter- and intramolecular KIE studies on the C^2–C^6/ene cyclization of enyne–allenes possessing ^{t}Bu, TMS, TIPS, and *p*-anisyl groups as substituents[4] because the experimental inter- and intramolecular KIEs clearly deviate from the statistically expected ratios. For example, near-unity intramolecular KIEs, constant over a wide range of temperature, are observed for enyne–allenes with a radical-stabilizing group at the allene terminus. The observed near-unity intramolecular KIE is explained using Carpenter's dynamic model[8a,29] suggesting that an intermediate with large energy excess may directly collapse into the products. Thus, with radical-stabilizing groups at the alkyne terminus a stepwise mechanism will prevail and nonstatistical dynamic effects become important. These mechanistic interpretations are in good agreement with earlier trapping reactions.[17a,21] On the other hand, if the enyne–allene is equipped with aryl groups at both termini (R^1, R^2 = aryl), the diradical intermediate finds itself in a deeper energy well and the overall reaction follows a classical stepwise mechanism as evidenced by significant intramolecular KIEs.

An alternative thermal cyclization mode of enyne–allenes is the C^2–C^6/DA reaction that requires an additional double bond, generally embedded in a benzene ring, at the allene terminus of **1** (R^2 or R^3 = Ar). When the process was first described,[17b] the almost identical reaction rates for **10** → **11** and **12** → **13** were taken as convincing evidence for a stepwise diradical mechanism (Scheme 3) because concerted DA cycloaddition of dienes involving aromatic subunits are usually dramatically decelerated by *ortho*-substituents. Finally, rearomatization of **13** via stepwise [1,5]-hydrogen shifts provides the fluorene derivative **14**. In the case of DA product **11**, the [1,5]-shift is prohibited leading to an overall reaction stop.[17b]

In contrast, DFT calculations from Ho et al.[30] on the parent enyne–allene **1** (with R^1 = R^2 = H, R^3 = vinyl, non-benzannulated) support a concerted mechanism for the C^2–C^6/DA reaction (Scheme 4). The new data presented here will furnish evidence that the thermal C^2–C^6/DA reaction takes place at the borderline between a stepwise and concerted process, with the stepwise mechanism being strongly influenced by nonstatistical dynamic effects. Moreover, we demonstrate

Scheme 3. Thermolyses of Mesityl- and Phenyl-Substituted Enyne–allenes[17b]

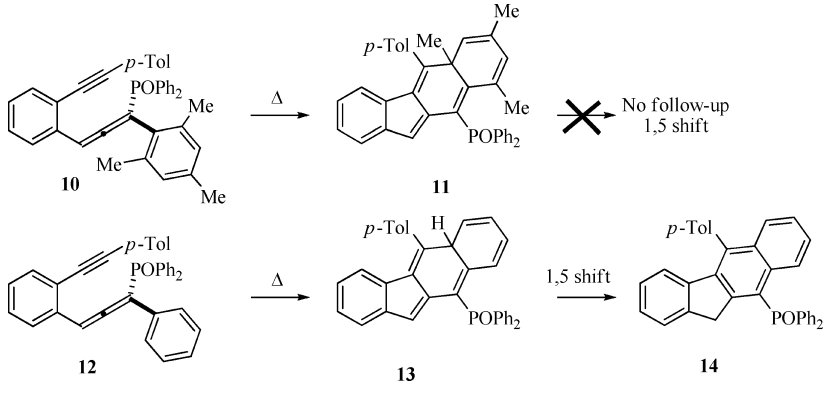

dx.doi.org/10.1021/jo302524a | J. Org. Chem. 2013, 78, 1451–1462

Scheme 4. Mechanistic Options for the Thermal C^2-C^6/DA Reaction of Enyne−Allenes

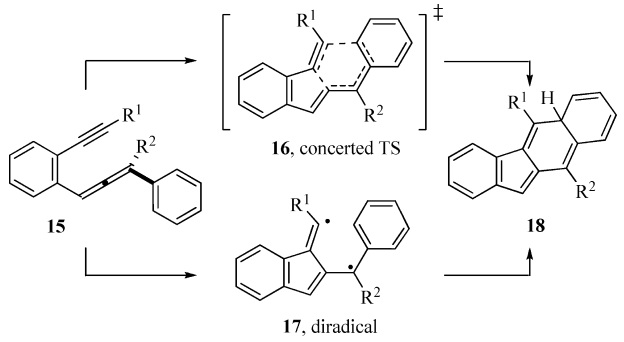

that substituents at the alkyne terminus affect nonstatistical aspects like in the case of C^2-C^6/ene reaction.[4,27]

RESULTS

Synthesis. As model compounds for our study we selected enyne−allenes **19**. The presence of an aryl substituent at the alkyne terminus is expected to steer the reaction toward the C^2-C^6 diradical pathway, whereas the *m*-tolyl subunit at the allene terminus should allow the diradical to divert into two constitutionally different benzofluorenes. If dynamic effects are present, the product ratio **20**/**21** (Scheme 5) should be temperature-independent.[8a]

The required enyne−allenes **19** for our experimental studies were obtained via a convenient four-step synthesis, starting out with a Sonogashira coupling of the corresponding alkyne with *o*-iodobenzaldehyde **22**[31] in the presence of a catalytic amount of palladium(II) affording **23a−e**.[32] The latter were treated with trimethylsilylacetylene in a Grignard reaction furnishing propargyl alcohols **24a−e** in good to excellent yields[17d,33] (Scheme 6). Compounds **24a−e** were treated with acetic anhydride in the presence of DMAP and NEt_3 to afford the corresponding propargyl acetates **25a−e**[34] that were subsequently reacted with *m*-tolylmagnesium bromide in the presence of $ZnCl_2$ and Pd(0) to yield **19a−e** in good to excellent yields.[35]

As an additional model compound, we selected enyne−allene **19f** in order to evaluate the effect of $P(O)Ph_2$, a radical-stabilizing unit (Scheme 7). Preparation of **19f** was achieved by reacting aldehyde **23a** with *m*-tolylacetylene to furnish propargyl alcohol **26** in very good yield. Finally, **26** was reacted with chlorodiphenylphosphine in the presence of NEt_3 to afford the diphenylphosphine oxide substituted enyne−allene **19f** in moderate yield.[17d]

All compounds were purified by flash column chromatography and characterized by ^1H, ^{13}C NMR, IR, and either HR-MS or elemental analysis. For example, the disappearance of the CH_3CO_2- signal in the ^1H NMR of **25a** at 2.09 ppm and subsequent manifestation of a singlet allene proton signal (3-H) at 7.37 ppm confirms the formation of enyne−allene **19a**. Moreover, in the reaction of **25a** to **19a** the alkyne carbon signal (C2) shifts from 102.3 to 210.4 ppm, the latter shift being diagnostic for enyne−allenes. The structural identity of all other enyne−allenes **19b−f** was confirmed analogously. Equally typical for **19** is an IR C═C═C stretching absorption around 1910−1931 cm^{-1}.

Thermolysis. As stated above, a temperature-independent product ratio may be taken as an important experimental indicator for dynamic behavior.[8a,36] Thermolysis of enyne−allenes **19a−f** was thus performed in dry degassed toluene in a sealed tube at various temperatures using a thermostat operating at a temperature stability of ±0.1 °C. Temperatures were selected on the basis of differential scanning calorimetry (DSC) onset temperatures of the exothermic signal responsible for cyclization. For example, with the onset temperature of **19f** being 53 °C, partial conversion was studied up to 90 °C. At this temperature, the conversion is 98% after 7 min of thermolysis. For the other cases (**19a−e**), the onset temperatures range from 86 to 103 °C, allowing partial conversion between 50 and 120 °C to be achieved. For **19a−e**, the thermolyses were initially performed at 50 °C for 60 min leading to 4−12% conversion, which is sufficient to measure integrations in the ^1H NMR with the desired accuracy. The conversion was 86−94% after 15 min at 120 °C. The thermal stability of products **20** and **21** obtained in the thermolysis was checked by heating them in dry toluene for sufficient time at the highest used temperature. All of them proved to be stable.

It proved to be very difficult to separate the constitutionally isomeric products **20** and **21**, but finally at least **20f** and **21f** were separated by preparative TLC. Their full characterization was accomplished by IR, HR-MS, ^1H, ^{13}C, and $^1H-^1H$ COSY NMR. In the $^1H-^1H$ COSY NMR, the single correlation of the methyl protons 8-H (see Scheme 8) at 2.18 ppm with the aromatic doublet for 9-H at 8.05 ppm confirms the formation of **21f**, whereas the methyl protons 1-H at 2.05 ppm correlate with a doublet of the aromatic proton 2-H at 7.13 ppm, thus supporting the formation of **20f**. All other constitutionally isomeric products, **20** and **21**, obtained after thermal cyclization of enyne−allenes **19a−e**, were isolated by preparative TLC and characterized in the mixture utilizing the same techniques. In the $^1H-^1H$ COSY spectra of the pure mixture of **20d** and **21d**, for example, a correlation of the singlet for proton 8-H at 2.38 ppm with the singlet signal of 9-H situated at 8.27 ppm arising from the naphthalene ring confirms the identity of **21d** (see the Supporting Information for complete $^1H-^1H$ correlation). By additionally considering integration, it is clear that singlet signals in ^1H NMR at 3.99 ppm and 4.01 ppm originate due to fulvenyl protons (5-H and 10-H) of **20d** and **21d**, respectively. Hence, the product ratios after thermolysis were determined by utilizing the integration of these two fulvenyl proton signals. In an analogous way, product ratio analysis and characterization were performed for other mixtures.

An evaluation of the product ratios **20a−c**/**21a−c** suggests that with increasing donor substitution at the phenyl group of

Scheme 5. Probing the Diels−Alder Cyclization of 19 for Nonstatistical Dynamic Effects via Formation of Two Products

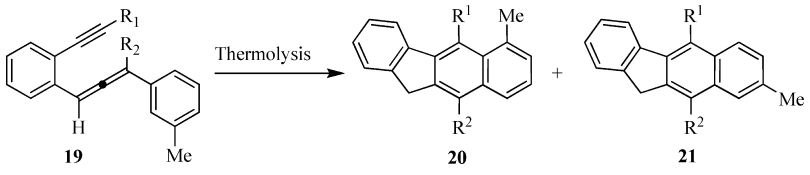

dx.doi.org/10.1021/jo302524a | J. Org. Chem. 2013, 78, 1451−1462

Scheme 6. Synthesis of Enyne−allenes 19a−e

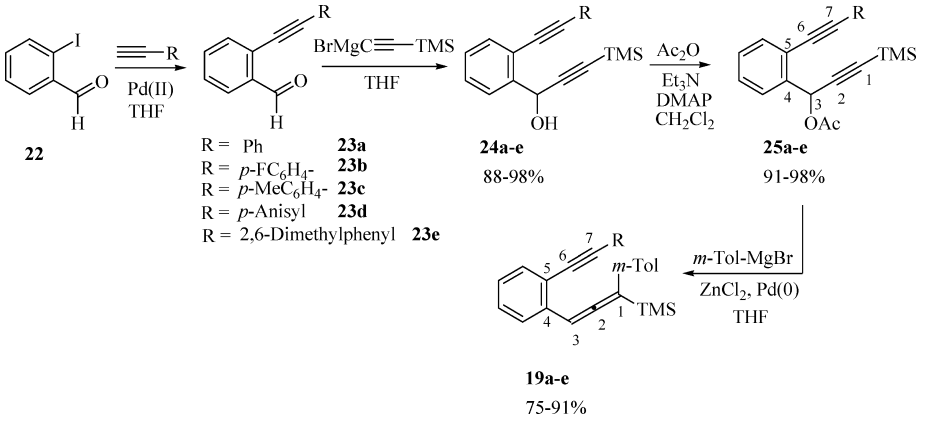

Scheme 7. Synthesis of Enyne−Allene 19f

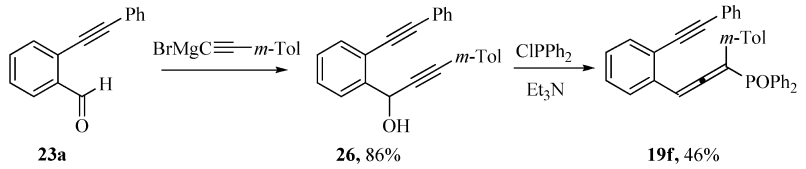

Scheme 8. Thermolyses of Enyne−Allenes 19a−f

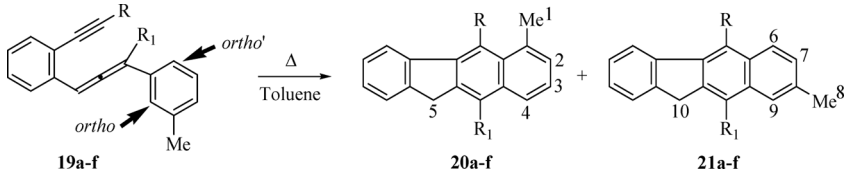

the alkyne terminus temperature independence is manifest at higher temperature. For **20d,e**/**21d,e** the product ratios are no longer constant within the given temperature window.

Computations. To further understand the thermal enyne−allene cyclization via stepwise and concerted pathways, reaction profiles were computed using DFT. By comparing the most common DFT methods in regard to accuracy and computational cost for the Bergman and Myers-Saito biradical cyclizations, Schreiner et al.[37] recommended the pure DFT functional (MPWLYP, G96LYP, and BLYP) as the most suitable methods with a 6-31G (d) basis set. Therefore, the BLYP[38] method with a 6-31G (d)[39] basis set was chosen for the stationary point calculations in the present study. Geometry optimizations of all gas-phase stationary points were performed with a 6-31G (d) basis set using Becke's pure gradient-corrected exchange functional in conjunction with the Lee−Yang−Parr nonlocal correlation functional (BLYP) as implemented in Gaussian 03.[40] Unrestricted calculations with a broken spin symmetry approach (BS-UBLYP), involving the mixing of the frontier molecular orbitals (HOMO and LUMO) to break the spin and spatial symmetries, were performed for the open-shell singlet state transition state (TS) structures and intermediates. In contrast, the restricted method was applied for all closed-shell molecules. It is well-known that the broken spin approach in combination with DFT provides good results for the cyclization of unsaturated systems.[17e,18e,f,41] The spin projection method of Yamaguchi et al.[42] was applied for molecules possessing spin contaminated wave functions. Calculated minima and first-order saddle point structures were verified by analyzing the harmonic vibrational frequencies via their analytical second derivatives because they should have NIMAG = 0 and 1, respectively. IRC calculations were carried out at the same level of theory to show that optimized transition states are connected to two minima on the energy hypersurface. Free energies including unscaled zero point vibrational energies after thermal correction are given in kcal mol^{-1} relative to the corresponding starting materials.

DISCUSSION

Statistical Kinetics Vs Nonstatistical Dynamics. According to previous experimental and theoretical studies, enyne-allenes **19a−f** are expected to undergo Schmittel cyclization via the corresponding diradical intermediate.[17,18] The diradical may either attack onto the *ortho* or *ortho′* positions of the *m*-tolyl subunit at the allene terminus along two pathways that according to statistical kinetic models should exhibit different activation enthalpies because of their constitutional and steric difference. After cyclization, the two constitutionally different benzofluorenes **20a−f** and **21a−f** should form.

Experimentally, the following picture arises: as shown in Table 1, the product ratios **20a,b**/**21a,b** prove to be temperature independent in the range 50−70 or 80 °C but decrease gently upon increasing the temperature up to 120 °C. Temperature independence of the product ratio is only to be explained in two ways: (1) Due to the relation $\ln (k_{20}/k_{21}) = -\Delta\Delta H^{\ddagger}/RT + \text{const}$ it requires $\Delta\Delta H^{\ddagger} = 0$. An accidential occurrence of $\Delta\Delta H^{\ddagger} = 0$, however, is extremely unlikely as the two competing reactions are of the same kind, with one being

dx.doi.org/10.1021/jo302524a | J. Org. Chem. 2013, 78, 1451−1462

Table 1. Product Ratios (20/21) from the Thermolysis of Enyne–Allenes 19a–f

	temp (°C)	time (min)	ratio[a] 20/21		temp (°C)	time (min)	ratio[a] 20/21
19a	50	60	1.76	**19b**	50	60	1.71
	60	55	1.76		60	55	1.71
	70	45	1.76		70	45	1.71
	80	35	1.66		80	35	1.71
	90	30	1.64		90	30	1.68
	100	25	1.61		100	25	1.66
	110	20	1.58		110	20	1.58
	120	15	1.56		120	15	1.51
19c	50	60	1.93	**19d**	50	60	1.88
	60	55	1.81		60	55	1.81
	70	45	1.77		70	45	1.73
	80	35	1.70		80	35	1.70
	90	30	1.65		90	30	1.61
	100	25	1.58		100	25	1.59
	110	20	1.58		110	20	1.57
	120	15	1.58		120	15	1.56
19e	50	60	1.88	**19f**	50	25	0.82
	60	55	1.84		60	20	0.82
	70	45	1.78		70	15	0.82
	80	35	1.76		80	10	0.83
	90	30	1.71		90	7	0.83
	100	25	1.68				
	110	20	1.63				
	120	15	1.61				

[a]Obtained from the crude ^{1}H NMR spectra. T_{onset} (DSC) = 86 °C (**19a**), 103 °C (**19b**), 85 °C (**19c**), 87 °C (**19d**), 90 °C (**19e**), and 53 °C (**19f**). Standard deviation of ratios = ±0.01–0.03.

clearly sterically disfavored in the product forming step. (2) As the ring-closure reactions should have different activation barriers ($\Delta\Delta H^{\ddagger} \neq 0$), the constant value may rather be attributed to dynamic effects.

To shed some light onto the various pathways, the energetics of the cyclization was calculated along the two possible pathways, stepwise and concerted, using the DFT method.

In the stepwise pathway of **19a**, the C^2–C^6 cyclization transition state, **19aa**‡, is located at 16.27 kcal mol^{-1} and thus lies 3.97 kcal mol^{-1} above the open-shell singlet diradical intermediate **19ab** (Figure 1). In the next step, the diradical may close in an intramolecular fashion either at the more hindered *ortho*-position with its nearby methyl group or less hindered *ortho*-position of the *m*-tolyl ring. The transition states corresponding to the more (**19ad**‡) and less (**19ac**‡) hindered *ortho* attack lie only 0.88 and 0.51 kcal mol^{-1}, respectively, above the σ,π-diradical intermediate **19ab**. Thus, when reactants pass from the highly energetic initial transition state into the shallow minima of **19ab** on the potential energy hypersurface, reaction dynamics may affect the selectivity due to the shallow minimum. Product formation is now a result of direct continuation of the trajectories that pass through the initial transition state.[9a,43] Molecules possessing enough energy along the initial vibration in the C^2–C^6 transition state will overcome the follow-up DA TS before IVR takes place, thus furnishing a product under nonstatistical dynamic conditions. In **19a**, the distance between C-7 and *ortho* and *ortho*′ carbon centers is 4.180 and 5.568 Å, respectively, which changes to 3.689 and 4.333 at the C^2–C^6 TS as well as to 3.359 and 3.399 Å for the diradical intermediate **19ab**, respectively. It is seen that C-7 is always closer to the *ortho* than the *ortho*′ center during the stepwise reaction course of **19a–c** (See Figure 2). Thus, the close proximity of the σ-radical center (C-7 atom) to the more hindered *ortho*-position is already preinstated in the C^2–C^6 transition state and kept in the σ,π-diradical intermediate. Importantly, the diradical with the opposite orientation, i.e., with the less hindered *ortho*′ carbon center being closer to C-7, does not show up as energetic minimum. Therefore, intramolecular radical combination occurs to a larger extent at the more hindered *ortho* site although it goes along with a higher transition state energy barrier than the less hindered attack.

In the concerted pathway, the two transition states have an energy barrier of 17.25 and 18.37 kcal mol^{-1} for the less (**19ag**‡) and more (**19ah**‡) hindered attack, i.e., *ortho*′ and *ortho* attack, respectively. While these barriers are slightly higher than those of the stepwise mechanism, it seems likely that with increasing temperatures (>70 °C) small amounts of reactant molecules are able to overcome them. As a consequence, the product ratio becomes increasingly temperature dependent. In agreement of theory and experiment, product **21a**, which results from the less hindered *ortho*′ attack, increases in the product ratio at >70 °C (see Table 1).

Replacing the phenyl group by a *p*-fluorophenyl group in **19b** gives rise to a similar minimum energy path (MEP) as for **19a**. In this case, the more and less hindered concerted transition states lie 0.95 and 0.66 kcal mol^{-1} higher in energy, respectively, than those of **19a**. Notably, the difference between transition state energies of the C^2–C^6 (**19ba**‡) and low-lying concerted route (**19bg**‡) is 0.72 kcal mol^{-1} higher than that for **19a**. Hence, the molecules are expected to need a higher temperature to realize some trajectories through the concerted pathway. Indeed, formation of a temperature-dependent product ratio starts at >80 °C.

Compound **19c** with a *p*-tolyl group at the alkyne terminus shows a different behavior because it exhibits a temperature-dependent product ratio from 50 to 100 °C. As such, one is led to assume that **19c** is not subjected to nonstatistical dynamics. Notably, though, product **20c**, which arises from the more hindered *ortho*-attack, forms in major amounts suggesting a nonclassical behavior. In this system, the difference between transition state energy of the C^2–C^6 (**19ca**‡) and the less hindered concerted route (**19cg**‡) is only 0.22 kcal mol^{-1}. Such finding is in full agreement with a temperature-dependent product ratio even at lower temperature.

Although no further computational study have been performed, the temperature-dependent product outcome from **19d,e** in the investigated temperature window can now readily be rationalized: (1) The intermediate wells are deeper for both cases, because the *p*-anisyl group (**19d**) stabilizes the intermediate to a larger extent than others and the 2,6-dimethylphenyl group (**19e**) increases the second TS barriers along the stepwise pathway by imparting an additional steric hindrance due its two methyl groups. These affect the product outcome at lower temperatures. (2) The energy gaps between C^2–C^6 TS and concerted TSs are expected to be small, which lead to the temperature dependent product formation also at higher temperatures.

Experimentally, replacement of the TMS by a $POPh_2$ group results in a preference for *ortho*′ attack and a constant product ratio at 50–90 °C. For the $POPh_2$-substituted enyne–allene, we compute the two singlet diradical intermediates **19fb** and **19fb1**,[44] but only one preceding C^2–C^6 TS. This TS is

dx.doi.org/10.1021/jo302524a | J. Org. Chem. 2013, 78, 1451–1462

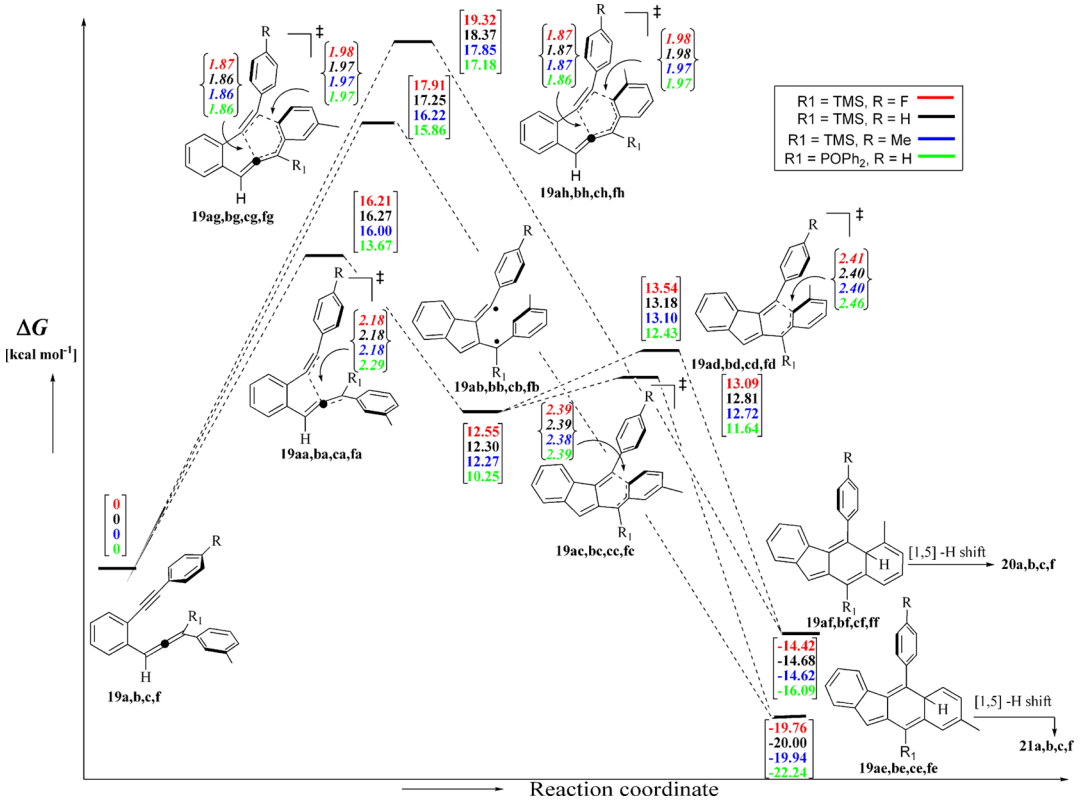

Figure 1. Reaction profiles for the thermal cyclization of **19a,b,c,f** in the gas phase at the (BS)-(U)/BLYP/6-31G(d) level. Bond distances (Å) and relative free energies after thermal correction are shown in second and third brackets, respectively. Numerical values in black, red, blue, and green correspond to **19a,b,c,f**.

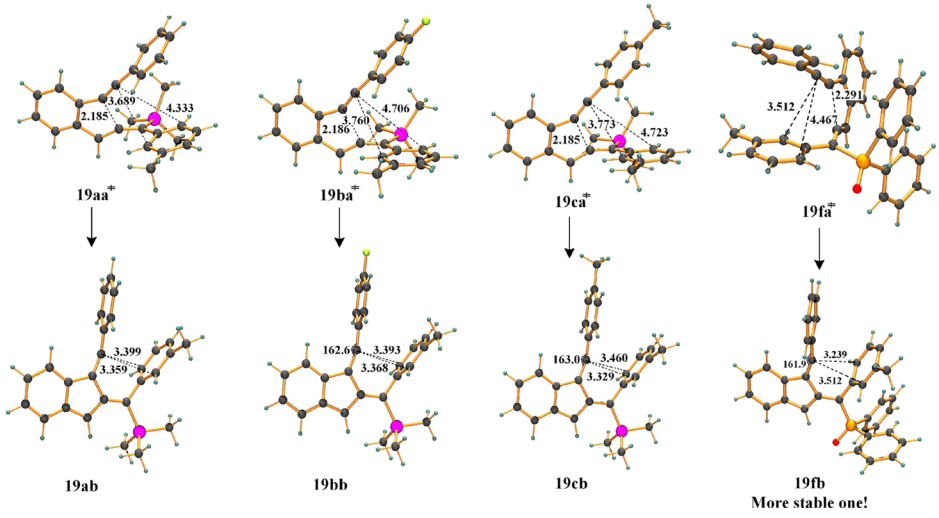

Figure 2. Three-dimensional presentation of the stationary points (C^2–C^6 transition states and intermediates) of **19a–c,f** showing distances in Å.

characterized by the more hindered *ortho* carbon center being closer to the C-7 atom. In contrast, the singlet diradical **19fb** with the less hindered *ortho′* carbon center being closer to C-7 is 0.65 kcal mol^{-1} lower in energy than **19fb1** that has the more hindered *ortho* carbon center closer to the C-7 atom. This finding suggests that there is a bifurcation and that the C^2–C^6 TS serves both intermediates. The computed relative energies of both intermediates are in good accordance with the experimentally detected product ratio. Moreover, as the $POPh_2$ unit is a radical stabilizing group, the C^2–C^6 TS to diradicals **19fb** and **19fb1** is significantly lower than the TS of the concerted route. As a result, the reaction proceeds exclusively via the stepwise pathway, showing no temperature dependence even at higher temperatures.

Stability and Character of Diradical. The DFT calculations show that the α-SOMO representing the σ radical is located at the aryl group of the alkyne terminus and the β-SOMO representing the π-radical is located at the fulvenyl moiety including the probing aryl ring. Because the energy difference between the singlet and triplet diradical states of **19ab** amounts to only 0.25 kcal mol^{-1} we see an almost 50% spin-contaminated state. The easiness of spin contamination

dx.doi.org/10.1021/jo302524a | J. Org. Chem. 2013, 78, 1451–1462

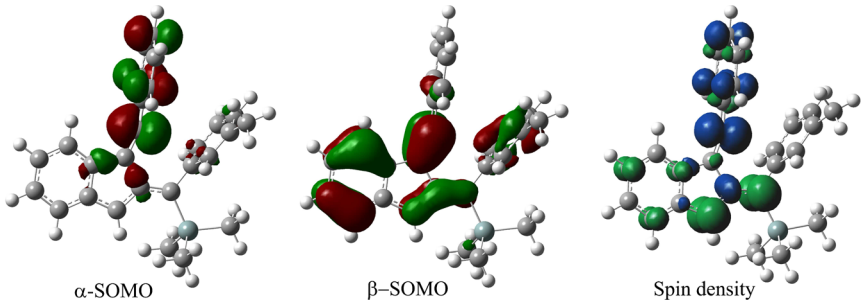

Figure 3. Two singly occupied molecular orbitals and spin density of **19ab** (singlet).

can be visualized from the spin density diagram in Figure 3. The amount of spin contamination of **19ab** was checked in solvents of different polarity, such as acetonitrile, acetone, dichloromethane and toluene, using PCM model as described by Houk et al..[45] The almost constant spin value of 1.029 in solvents of different polarity suggests that the diradical under investigation is nonpolar.

CONCLUSIONS

Herein we present examples in which the changeover between temperature-dependent and -independent product ratios in the thermal Schmittel (C^2–C^6)/DA cyclization of various substituted enyne-allenes occurs as a function of an remote electronic substituent. The scenario is being investigated experimentally and computationally with DFT. The cyclization process occurs through a nonpolarized σ,π-diradical intermediate for enyne allenes containing an aryl group at the alkyne terminus. In most cases, *i.e.* **19a–c**, nonstatistical dynamics explains the selectivity of product formation and the constant product ratio at low temperature (50 to 70 or 80 °C). At medium temperature range (70 or 80 °C to 120 or 130 °C), the product ratios are not constant any more and the selectivity of product formation decreases, because of increasing amounts of product molecules taking the classical concerted pathway.

EXPERIMENTAL SECTION

General Methods. All commercially available reagents and NMR solvents were used without further purification. Reactions were carried out under nitrogen atmosphere using freshly distilled, anhydrous solvents. Diethyl ether was first dried over calcium hydride and then distilled over sodium. Tetrahydrofuran (THF) and toluene were distilled over potassium. Triethylamine (NEt_3) and dichloromethane (DCM) were distilled over calcium hydride. All reactions were followed by thin-layer chromatography (TLC) on silica gel plates (60F-254). Silica gel (0.035–0.070 mm) was used for column chromatography. Preparative TLC was carried out by using silica gel plates (60 F_{254}). ^{1}H and ^{13}C NMR spectra were recorded on a 400 MHz spectrometer using the deuterated solvent as the lock and residual solvent as internal reference. Chemical shifts (δ) are reported in ppm. The following abbreviations were utilized to describe NMR peak patterns: s = singlet, d = doublet, t = triplet td = triplet of doublets, dd = doublet of doublets, ddd = doublet of doublet of doublets, m = multiplet, and brs = broad singlet. Coupling constants refer to proton–proton coupling unless mentioned otherwise. The numbering of the carbon skeleton of molecular formulas in the manuscript does not comply with IUPAC nomenclature rules; it is only used for assignments of the NMR spectra. Compounds **23e**, **24a–e**, **25a–e**, and **26** were characterized by IR, ^{1}H, ^{13}C NMR, and HR-MS (linear ion trap analyzer) or elemental analysis, whereas **19a–f**, **20a–f**, and **21a–f** were characterized using ^{1}H–^{1}H COSY NMR in addition. 2-Iodobenzaldehyde (**22**),[31] 2-(phenylethynyl)benzaldehyde (**23a**),[32a] 2-((4-fluorophenyl)ethynyl)benzaldehyde (**23b**),[46] 2-(*p*-tolylethynyl)benzaldehyde (**23c**),[17d] 2-(4-anisylethynyl)benzaldehyde-(**23d**),[47] and 3-(trimethylsilyl)-1-[2-(2-phenylethynyl)phenyl]prop-2-yn-1-ol (**24a**)[48] were synthesized according to reported procedures.

2-((2,6-Dimethylphenyl)ethynyl)benzaldehyde (23e). 2-Ethynyl-1,3-dimethylbenzene (800 mg, 6.14 mmol) was added to a mixture of 2-iodobenzaldehyde (**22**) (713 mg, 3.07 mmol), CuI (41.0 mg, 215 μmol), $[Pd(PPh_3)_2]Cl_2$ (60.0 mg, 86.2 μmol), and 2 mL of triethylamine. After being stirred for 16 h at room temperature, the reaction mixture was quenched with saturated aqueous ammonium chloride solution. The aqueous layer was washed three times with *n*-pentane. The combined organic layers were dried over sodium sulfate and evaporated under reduced pressure. After purification by flash column chromatography (silica gel, *n*-hexane/ethyl acetate = 98:2, R_f = 0.28) compound **19e** (651 mg, 91%) was isolated as a white solid: mp = 59 °C; IR (KBr) $\tilde{\nu}$ 3061, 2858, 2823, 2388, 2279, 1699, 1618, 1595, 1550, 1454, 1388, 1330, 1162, 813, 772 cm^{-1}; ^{1}H NMR (400 MHz, C_6D_6) δ 2.36 (s, 6H), 6.82–6.86 (m, 3H), 6.92–6.97 (m, 2H), 7.31 (ddd, J = 7.8, 1.2, 0.4 Hz, 1H), 7.88 (ddd, J = 7.8, 1.2, 0.4 Hz, 1H), 10.77 (d, J = 0.7 Hz, 1H) ppm; ^{13}C NMR (100 MHz, C_6D_6) δ 21.5, 94.2, 94.8, 123.0, 127.5, 127.5, 127.9, 128.8, 129.1, 133.6, 133.7, 136.6, 141.2, 190.7 ppm. Anal. Calcd for $C_{17}H_{14}O$: C, 87.15; H, 6.02. Found: C, 87.11; H, 6.00.

General Procedure for Preparation of Propargyl Alcohol (24a–e). A solution of ethylmagnesium bromide (6.98 mmol), prepared from ethyl bromide (0.520 mL, 6.98 mmol) and magnesium turnings (167 mg, 6.98 mmol) in 50 mL of dry tetrahydrofuran was added to a solution of the monosubstituted acetylene (7.68 mmol) in 20 mL of dry tetrahydrofuran under nitrogen atmosphere at 0 °C. The resulting reaction mixture was stirred at room temperature for 15 min to exchange the Grignard with acetylene followed by the addition of a solution of aldehyde (6.28 mmol) in dry tetrahydrofuran (10 mL). After being stirred for another 15 min at room temperature, the reaction mixture was quenched with water. The aqueous layer was extracted three times with diethyl ether. The combined organic layers were dried over $MgSO_4$ and concentrated to furnish the crude product. The crude products were then subjected for flash column chromatography on silica gel to yield the pure products.

1-(2-((4-Fluorophenyl)ethynyl)phenyl)-3-(trimethylsilyl)-prop-2-yn-1-ol (24b). Column chromatography, *n*-hexane/ethyl acetate (17:3), R_f = 0.51, colorless oil: 94% yield (5.90 mmol, 1.90 g); IR (KBr) $\tilde{\nu}$ 3541, 3401, 3068, 2960, 2899, 2173, 1597, 1509, 1408, 1232, 1156, 1094, 1038, 982, 847, 760 cm^{-1}. ^{1}H NMR (400 MHz, C_6D_6) δ = 0.09 (s, 9H), 2.26 (d, J = 5.8 Hz, 1H), 6.00 (d, J = 5.8 Hz, 1H), 6.64 (t, J = 8.8 Hz, J_{H-F} = 8.8 Hz, 2H), 6.89 (td, J = 7.8, 1.2 Hz, 1H), 7.01 (td, J = 7.8, 1.2 Hz, 1H), 7.24 (dd, J = 8.8 Hz, J_{H-F} = 5.4 Hz, 2H), 7.41 (dd, J = 7.8, 1.2 Hz, 1H), 7.74 (ddd, J = 7.8, 1.2, 0.4 Hz, 1H) ppm; ^{13}C NMR (100 MHz, C_6D_6) δ −0.2, 63.8, 87.2, 90.7, 94.4, 106.0, 115.9 (d, J_{C-F} = 22.2 Hz), 119.5 (d, J_{C-F} = 3.3 Hz), 121.7, 127.0, 128.3, 129.2, 132.5, 133.8 (d, J_{C-F} = 8.1 Hz), 143.2, 163.0 (d, J_{C-F} = 247.9 Hz) ppm; HRMS-EI (m/z) for $C_{20}H_{19}FOSi$ [M]$^+$ calcd 322.119, found 322.119.

1-(2-(4-Tolylethynyl)phenyl)-3-(trimethylsilyl)prop-2-yn-1-ol (24c). Column chromatography, *n*-hexane/ethyl acetate (9:1), R_f = 0.47, yellow oil: 92% yield (5.78 mmol, 1.84 g); IR (KBr) $\tilde{\nu}$ 3544, 3420, 3066, 3029, 2960, 2898, 2216, 2173, 1598, 1511, 1250, 1038, 982, 851, 759 cm^{-1}; ^{1}H NMR (400 MHz, C_6D_6) δ = 0.10 (s, 9H), 1.99

dx.doi.org/10.1021/jo302524a | J. Org. Chem. 2013, 78, 1451–1462

(s, 3H), 2.18 (d, J = 5.6 Hz, 1H), 6.05 (d, J = 5.6 Hz, 1H), 6.85 (d, J = 8.0 Hz, 2H), 6.88 (td, J = 7.8, 1.2 Hz, 1H), 7.00 (td, J = 7.8, 1.2 Hz, 1H), 7.44 (dd, J = 7.8, 1.2 Hz, 1H, semicovered), 7.46 (d, J = 8.0 Hz, 2H, semicovered), 7.74 (ddd, J = 7.8, 1.2, 0.4 Hz, 1H) ppm; ^{13}C NMR (100 MHz, C_6D_6) δ −0.1, 21.3, 63.9, 87.0, 90.5, 95.9, 106.2, 120.6, 122.1, 126.8, 128.2, 128.8, 129.4, 131.9, 132.4, 138.8, 143.1 ppm; HRMS-EI (m/z) for $C_{21}H_{22}OSi$ $[M]^+$ calcd 318.144, found 318.143.

1-(2-((4-Methoxyphenyl)ethynyl)phenyl)-3-(trimethylsilyl)-prop-2-yn-1-ol (24d). Column chromatography, *n*-pentane/dichloromethane (4:1), R_f = 0.56, yellow oil: 74% yield (4.65 mmol, 1.55 g); IR (KBr) $\tilde{\nu}$ 3442, 3068, 2959, 2899, 2838, 2215, 2172, 1607, 1511, 1250, 1175, 1033, 844, 760 cm^{-1}; ^{1}H NMR (400 MHz, C_6D_6) δ = 0.11 (s, 9H), 2.26 (d, J = 5.9 Hz, 1H), 3.18 (s, 3H), 6.08 (d, J = 5.9 Hz, 1H), 6.64 (d, J = 8.8 Hz, 2H), 6.89 (td, J = 7.8, 1.2 Hz, 1H), 7.00 (td, J = 7.8, 1.2 Hz, 1H), 7.45−7.48 (m, 3H), 7.75 (ddd, J = 7.8, 1.2, 0.4 Hz, 1H) ppm; ^{13}C NMR (100 MHz, C_6D_6) δ −0.1, 54.7, 64.0, 86.3, 90.5, 95.8, 106.2, 114.4, 115.6, 122.3, 126.9, 128.2, 128.7, 132.3, 133.4, 143.0, 160.3 ppm. Anal. Calcd for $C_{21}H_{22}O_2Si$: C, 75.41; H 6.63. Found: C, 75.18; H 6.66.

1-(2-((2,6-Dimethylphenyl)ethynyl)phenyl)-3-(trimethylsilyl)prop-2-yn-1-ol (24e). Column chromatography, *n*-pentane/dichloromethane (4:1), R_f = 0.64, yellow oil: 47% yield (2.95 mmol, 0.980 g); IR (KBr) $\tilde{\nu}$ 3540, 3442, 3092, 2960, 2918, 2893, 2215, 2172, 1607, 1511, 1250, 1175, 1033, 844, 760 cm^{-1}; ^{1}H NMR (400 MHz, C_6D_6) δ = 0.07 (s, 9H), 2.03−2.05 (m, 1H), 2.50 (s, 6H), 6.07 (d, J = 5.5 Hz, 1H), 6.90 (d, J = 7.6 Hz, 2H, semicovered), 6.91 (td, J = 7.8, 1.2 Hz, 1H, semicovered), 6.95−6.99 (m, 1H), 7.03 (td, J = 7.8, 1.2 Hz, 1H), 7.42 (dd, J = 7.8, 1.2 Hz, 1H), 7.80 (ddd, J = 7.8, 1.2, 0.6 Hz, 1H) ppm; ^{13}C NMR (100 MHz, C_6D_6) δ −0.2, 21.4, 63.8, 90.7, 93.3, 95.7, 106.1, 122.4, 123.3, 126.7, 127.2, 128.2, 128.4, 128.9, 132.7, 140.7, 142.6 ppm. Anal. Calcd for $C_{22}H_{24}OSi$: C, 79.47; H, 7.28. Found: C, 79.40; H, 7.31.

1-(2-(Phenylethynyl)phenyl)-3-*m*-tolylprop-2-yn-1-ol (26). Column chromatography, *n*-hexane/ethyl acetate (3:2), R_f = 0.75, viscous yellow oil: 88% yield (5.53 mmol, 1.78 g); IR (KBr) $\tilde{\nu}$ 3391, 3059, 3032, 2920, 2860, 2226, 1600, 1493, 1448, 1378, 1270, 1094, 1033, 998, 972, 908, 785, 757, 733; ^{1}H NMR (400 MHz, C_6D_6) δ = 1.89 (s, 3H), 2.39 (brs, 1H), 6.27 (d, J = 5.5 Hz, 1H), 6.77 (d, J = 7.6 Hz, 1H), 6.87 (t, J = 7.6 Hz, 1H), 6.92 (td, J = 7.8, 1.3 Hz, 1H), 6.96−7.00 (m, 3H), 7.05 (td, J = 7.8, 1.3 Hz, 1H), 7.18 (s, 1H), 7.24 (d, J = 7.6 Hz, 1H), 7.47−7.51 (m, 3H), 7.81 (d, J = 7.8 Hz, 1H) ppm; ^{13}C NMR (100 MHz, C_6D_6) δ 20.6, 63.9, 86.6, 87.6, 89.5, 95.6, 121.9, 123.2, 123.6, 127.0, 128.2, 128.4, 128.6(2C), 129.1, 129.1, 129.4, 131.9, 132.6, 132.8, 138.0, 143.6 ppm; HRMS-EI (m/z) for $C_{24}H_{18}O$ $[M]^+$ calcd 322.136, found 322.133.

General Procedure for the Preparation of Propargyl Acetates 25a−e. 4-(Dimethylamino)pyridine (174 mg, 1.43 mmol), acetic anhydride (0.840 mL, 8.91 mmol), and dry triethylamine (2 mL) were added to a stirred solution of propargyl alcohol (7.13 mmol) in dry dichloromethane. After being stirred for 30 min at room temperature, the reaction mixture was quenched and washed with saturated $NaHCO_3$ solution. The aqueous layer was extracted with dichloromethane three times. The combined organic layers were dried over $MgSO_4$ and concentrated under reduced pressure to produce the crude product. The resulting crude products were subsequently purified by flash silica gel column chromatography.

1-(2-(Phenylethynyl)phenyl)-3-(trimethylsilyl)prop-2-ynyl acetate (25a). Column chromatography, *n*-hexane/ethyl acetate (9:1), R_f = 0.54, dark yellow oil: 83% yield (5.92 mmol, 2.05 g); IR (KBr) $\tilde{\nu}$ 3064, 2961, 2900, 2217, 2181, 1744, 1495, 1370, 1225, 1045, 958, 911, 847 cm^{-1}; ^{1}H NMR (400 MHz, C_6D_6) δ 0.10 (s, 9H), 1.59 (s, 3H), 6.91 (td, J = 7.8, 1.2 Hz, 1H), 6.94−7.05 (m, 4H), 7.43 (dd, J = 7.8, 1.2 Hz, 1H), 7.50 (s, 1H), 7.65 (dd, J = 8.2, 1.5 Hz, 2H), 8.01 (dd, J = 7.8, 1.2 Hz, 1H) ppm; ^{13}C NMR (100 MHz, C_6D_6) δ −0.3, 20.3, 64.5, 86.9, 92.5, 95.6, 102.3, 123.3, 123.5, 128.5, 128.7, 128.8 (2C), 129.1, 132.1, 132.6, 138.9, 169.1 ppm; HRMS-EI (m/z) for $C_{22}H_{22}O_2Si$ $[M]^+$ calcd 346.139, found 346.139.

1-(2-((4-Fluorophenyl)ethynyl)phenyl)-3-(trimethylsilyl)-prop-2-ynyl Acetate (25b). Column chromatography, *n*-hexane/ethyl acetate (20:1), R_f = 0.47, colorless oil: 96% yield (6.84 mmol, 2.49 g); IR (KBr) $\tilde{\nu}$ 3069, 2960, 2181, 1743, 1597, 1509, 1369, 1224, 1159, 1044, 839, 760 cm^{-1}; ^{1}H NMR (400 MHz, C_6D_6) δ = 0.10 (s, 9H), 1.58 (s, 3H), 6.63 (t, J = 8.8 Hz, J_{H-F} = 8.8 Hz, 2H), 7.91 (td, J = 7.8, 1.2 Hz, 1H), 7.04 (td, J = 7.8, 1.2 Hz, 1H), 7.40−7.45 (m, 3H), 7.48 (s, 1H), 8.02 (dd, J = 7.8, 1.2 Hz, 1H) ppm; ^{13}C NMR (100 MHz, C_6D_6) δ −0.3, 20.6, 64.4, 86.6, 92.6, 94.7, 102.2, 115.9 (d, J_{C-F} = 21.8 Hz), 119.3 (d, J_{C-F} = 3.6 Hz), 123.3, 128.6, 128.9, 129.2, 132.5, 134.1 (d, J_{C-F} = 8.4 Hz), 138.9, 163.0 (d, J_{C-F} = 248.3 Hz), 169.1 ppm; HRMS-EI (m/z) for $C_{22}H_{21}FO_2Si$ $[M]^+$ calcd 364.129, found 364.130.

1-(2-(4-Tolylethynyl)phenyl)-3-(trimethylsilyl)prop-2-ynyl Acetate (25c). Column chromatography, *n*-hexane/ethyl acetate (20:1), R_f = 0.54, yellow oil: 92% yield (6.56 mmol, 2.36 g); IR (KBr) $\tilde{\nu}$ 3052, 2960, 2849, 2216, 2180, 1745, 1511, 1368, 1251, 1222, 1044, 845, 760 cm^{-1}; ^{1}H NMR (400 MHz, C_6D_6) δ = 0.11 (s, 9H), 1.60 (s, 3H), 1.96 (s, 3H), 6.84 (d, J = 8.0 Hz, 2H), 6.90 (td, J = 7.8, 1.2 Hz, 1H), 7.03 (td, J = 7.8, 1.2 Hz, 1H), 7.46 (dd, J = 7.8, 1.2 Hz, 1H), 7.56 (s, 1H), 7.62 (d, J = 8.0 Hz, 2H), 8.04 (dd, J = 7.8, 1.2 Hz, 1H) ppm; ^{13}C NMR (100 MHz, C_6D_6) δ −0.3, 20.3, 21.3, 64.6, 86.4, 92.5, 96.2, 102.4, 120.4, 123.8, 128.5, 128.6, 129.1, 129.5, 132.1, 132.5, 138.8 (2C), 169.1 ppm; HRMS-EI (m/z) for $C_{23}H_{24}O_2Si$ $[M]^+$ calcd 360.155, found 360.154.

1-(2-((4-Methoxyphenyl)ethynyl)phenyl)-3-(trimethylsilyl)-prop-2-ynyl Acetate (25d). Column chromatography, *n*-pentane/dichloromethane (5:1), R_f = 0.58, colorless oil: 90% yield (6.42 mmol, 2.42 g); IR (KBr) $\tilde{\nu}$ 3070, 2960, 2838, 2215, 2180, 1743, 1607, 1513, 1289, 1251, 1223, 1035, 845, 761 cm^{-1}; ^{1}H NMR (400 MHz, C_6D_6) δ = 0.11 (s, 9H), 1.61 (s, 3H), 3.16 (s, 3H), 6.61 (d, J = 8.8 Hz, 2H), 6.93 (td, J = 7.8, 1.2 Hz, 1H), 7.04 (td, J = 7.8, 1.2 Hz, 1H), 7.48 (dd, J = 7.8, 1.2 Hz, 1H), 7.57 (s, 1H), 7.63 (d, J = 8.8 Hz, 2H), 8.06 (dd, J = 7.8, 1.2 Hz, 1H) ppm; ^{13}C NMR (100 MHz, C_6D_6) δ −0.3, 20.4, 54.7, 64.6, 85.7, 92.5, 96.2, 102.4, 114.5, 115.4, 124.1, 128.3, 128.5, 129.1, 132.3, 133.7, 138.6, 160.4, 169.2 ppm. Anal. Calcd for $C_{23}H_{24}O_3Si$: C, 73.37; H, 6.42. Found: C, 73.44; H, 6.20.

1-(2-((2,6-Dimethylphenyl)ethynyl)phenyl)-3-(trimethylsilyl)prop-2-ynyl acetate (25e). Column chromatography, *n*-pentane/dichloromethane (5:1), R_f = 0.52, colorless oil: 94% yield (6.70 mmol, 2.51 g); IR (KBr) $\tilde{\nu}$ 3072, 2960, 2852, 2179, 1749, 1487, 1369, 1222, 1041, 957, 845, 761 cm^{-1}; ^{1}H NMR (400 MHz, C_6D_6) δ = 0.05 (s, 9H), 1.55 (s, 3H), 2.57 (s, 6H), 6.88 (d, J = 7.8 Hz, 2H), 6.92 (td, J = 7.8, 1.2 Hz, 1H), 6.93−6.97 (m, 1H), 7.04 (td, J = 7.8, 1.2 Hz, 1H), 7.43 (dd, J = 7.8, 1.2 Hz, 1H), 7.46 (s, 1H), 7.92 (d, J = 7.8 Hz, 1H) ppm; ^{13}C NMR (100 MHz, C_6D_6) δ −0.3, 20.3, 21.4, 64.8, 92.2, 93.6, 95.1, 102.6, 123.2, 123.6, 127.2 (2C), 128.5, 128.7, 128.9, 132.9, 138.9, 140.8, 168.8 ppm. Anal. Calcd for $C_{24}H_{26}O_2Si$: C, 76.96; H, 7.00. Found: C, 76.64; H 6.87.

General Procedure for Preparation of Enyne−Allenes 19a−e. *m*-Tolylmagnesium bromide solution (23.4 mmol, prepared by standard Grignard reaction) in dry tetrahydrofuran (50 mL) was added dropwise to a solution of zinc chloride (2.22 g, 16.4 mmol) in 20 mL of dry diethyl ether at room temperature under nitrogen atmosphere. The reaction mixture was stirred for 30 min to complete formation of the diarylzinc. Subsequently, the reaction mixture was cooled down to −60 °C followed by addition of tetrakis-(triphenylphosphine)palladium(0) (0.674 g, 0.584 mmol) in 10 mL of dry tetrahydrofuran. After stirring for 15 min at the same temperature, propargyl acetate (5.84 mmol) in dry tetrahydrofuran (10 mL) was added to the mixture. Finally, the solution was allowed to stir for 14 h to complete the reaction. The reaction mixture was quenched with saturated ammonium chloride solution. The aqueous layer was extracted three times with diethyl ether. The combined organic layers were dried over Na_2SO_4 and concentrated under reduced pressure. Flash silica gel column chromatography was utilized to obtain the pure compound.

Trimethyl(3-(2-(phenylethynyl)phenyl)-1-*m*-tolylpropa-1,2-dienyl)silane (19a). Column chromatography, *n*-hexane, R_f = 0.55, yellow oil: 91% yield (5.31 mmol, 2.01 g); IR (KBr) $\tilde{\nu}$ 3056, 3028, 2958, 2113, 1911, 1597, 1489, 1445, 1252, 1118, 1084, 949, 844, 756 cm^{-1}. ^{1}H NMR (400 MHz, C_6D_6) δ 0.29 (s, 9H, 9-H), 2.08 (s, 3H, 14-H), 6.86 (td, J = 7.8, 1.2 Hz, 1H, 5-H), 6.89 (d, J = 7.8 Hz, 1H, 11-H),

dx.doi.org/10.1021/jo302524a | J. Org. Chem. 2013, 78, 1451−1462

6.96−7.00 (m, 3H, 1, 2-H), 7.01 (td, J = 7.8, 1.2 Hz, 1H, 6-H), 7.11 (t, J = 7.8 Hz, 1H, 12-H), 7.28 (s, 1H, 8-H), 7.29 (d, J = 7.8 Hz, 1H, 13-H), 7.37 (s, 1H, 10-H), 7.42 (dd, J = 6.8, 2.4 Hz, 2H, 3-H), 7.52 (ddd, J = 7.8, 1.2, 0.4 Hz, 1H, 4-H), 7.65 (dd, J = 7.8, 1.2 Hz, 1H, 7-H) ppm; ^{13}C NMR (100 MHz, C_6D_6) δ −0.1, 21.4, 88.5, 90.0, 95.0, 105.2, 121.2, 123.7, 125.4, 126.0, 126.5, 127.9, 128.4, 128.6, 128.9, 129.0, 129.1, 131.9, 133.1, 136.6, 137.0, 138.5, 210.4 ppm. Anal. Calcd for $C_{27}H_{26}Si$: C, 85.66; H 6.92. Found: C, 85.73; H 6.84.

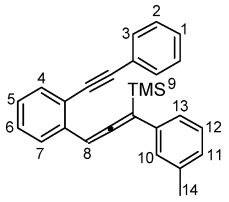

(3-(2-((*p*-Fluorophenyl)ethynyl)phenyl)-1-*m*-tolylpropa-1,2-dienyl)trimethylsilane (19b). Column chromatography, *n*-hexane/ethyl acetate (49:1), R_f = 0.61, yellow oil: 72% yield (4.20 mmol, 1.67 g); IR (KBr) $\tilde{\nu}$ 3058, 2956, 2924, 2855, 2215, 2179, 1911, 1601, 1508, 1230, 1155, 836, 755 cm^{-1}; ^{1}H NMR (400 MHz, C_6D_6) δ 0.29 (s, 9H, 8-H), 2.06 (s, 3H, 13-H), 6.58 (t, J = 8.8 Hz, J_{H-F} = 8.8 Hz, 2H, 1-H), 6.85 (td, J = 7.8, 1.2 Hz, 1H, 4-H), 6.89 (d, J = 7.8 Hz, 1H, 10-H), 7.00 (td, J = 7.8, 1.2, Hz, 1H, 5-H), 7.10 (t, J = 7.8 Hz, 1H, 11-H), 7.12 (dd, J = 8.8, 3.6 Hz, 2H, 2-H), 7.25 (s, 1H, 7-H), 7.31 (d, J = 7.8 Hz, 1H, 12-H), 7.39 (s, 1H, 9-H), 7.52 (dd, J = 7.8, 1.2 Hz, 1H, 3-H), 7.68 (dd, J = 7.8, 1.2 Hz, 1H, 6-H) ppm; ^{13}C NMR (100 MHz, C_6D_6) δ −0.1, 21.4, 88.0, 89.9, 93.8, 105.3, 115.7 (d, J_{C-F} = 22.1 Hz), 119.7 (d, J_{C-F} = 3.4 Hz), 121.0, 125.4, 126.0, 126.5, 128.9, 129.0, 129.0, 133.0 (2C), 133.7 (d, J_{C-F} = 8.2 Hz), 136.6, 137.0, 138.6, 162.8 (d, J_{C-F} = 247.7 Hz), 210.2 ppm; HRMS-EI (m/z) for $C_{27}H_{25}FSi$ [M]$^+$ calcd 396.171, found 396.171.

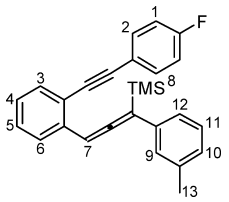

Trimethyl(1-*m*-tolyl-3-(2-(*p*-tolylethynyl)phenyl)propa-1,2-dienyl)silane (19c). Column chromatography, *n*-hexane/ethyl acetate (49:1), R_f = 0.48, yellow oil: 71% yield (4.15 mmol, 1.63 g); IR (KBr) $\tilde{\nu}$ 3052, 2959, 2214, 1910, 1600, 1509, 1481, 1250, 944, 842, 754 cm^{-1}; ^{1}H NMR (400 MHz, C_6D_6) δ 0.28 (s, 9H, 9-H), 1.97 (s, 3H, 1-H), 2.07 (s, 3H, 14-H), 6.80 (d, J = 8.0 Hz, 2H, 2-H), 6.85 (ddd, J = 8.0, 7.8, 1.0 Hz, 1H, 5-H), 6.89 (d, J = 7.8 Hz, 1H, 11-H), 7.00 (ddd, J = 8.0, 7.8, 1.0 Hz, 1H, 6-H), 7.11 (t, J = 7.8 Hz, 1H, 12-H), 7.31 (d, J = 7.8 Hz, 1H, 13-H), 7.34 (s, 1H, 8-H), 7.38−7.40 (m, 3H, 3,10-H), 7.56 (dd, J = 7.8, 1.0 Hz, 1H, 4-H), 7.68 (dd, J = 8.0, 1.0 Hz, 1H, 7-H) ppm; ^{13}C NMR (100 MHz, C_6D_6) δ −0.1, 21.3, 21.4, 87.9, 90.1, 95.2, 105.2, 120.9, 121.5, 125.5, 126.0, 126.5, 127.9, 128.8, 128.9, 129.1, 129.4, 131.9, 133.1, 136.7, 136.9, 138.4, 138.5, 210.4 ppm; HRMS-EI (m/z) for $C_{28}H_{28}Si$ [M]$^+$ calcd 392.196, found 392.196.

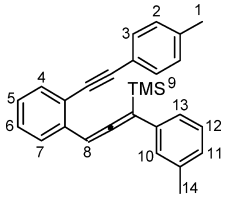

[3-[2-(*p*-Anisylethynyl)phenyl]-1-*m*-tolylpropa-1,2-dienyl]-trimethylsilane (19d). Column chromatography, *n*-pentane/dichloromethane (49:1), R_f = 0.38, yellow oil: 98% yield (5.72 mmol, 2.34 g); IR (KBr) $\tilde{\nu}$ 3061, 2956, 2840, 2280, 2213, 1911, 1606, 1510, 1288, 1249, 1174, 1033, 841, 756 cm^{-1}; ^{1}H NMR (400 MHz, C_6D_6) δ 0.29 (s, 9H, 9-H), 2.07 (s, 3H, 14-H), 3.16 (s, 3H, 1-H), 6.58 (d, J = 8.8 Hz, 2H, 2-H), 6.86 (td, J = 7.8, 1.2 Hz, 1H, 5-H), 6.89 (d, J = 8.0 Hz, 1H, 11-H), 7.01 (td, J = 7.8, 1.2 Hz, 1H, 6-H), 7.11 (t, J = 8.0 Hz, 1H, 12-H), 7.32 (d, J = 8.0 Hz, 1H, 13-H), 7.36 (s, 1H, 8-H), 7.38−7.40 (m, 3H, 3,10-H), 7.58 (ddd, J = 7.8, 1.2, 0.4 Hz, 1H, 4-H), 7.69 (dd, J = 7.8, 1.2 Hz, 1H, 7-H) ppm; ^{13}C NMR (100 MHz, C_6D_6) δ −0.1, 21.4, 54.7, 87.2, 90.2, 95.2, 105.2, 114.4, 115.9, 121.7, 125.5, 126.0, 126.5, 127.9, 128.7, 128.9, 129.1, 133.0, 133.4, 136.7, 136.8, 138.5, 160.2, 210.4 ppm. Anal. Calcd for $C_{28}H_{28}OSi$: C, 82.30; H, 6.91. Found: C, 82.05; H, 6.95.

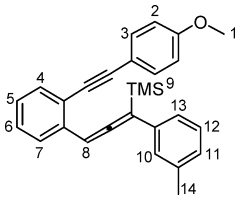

[3-[2-(2,6-Dimethylphenylethynyl)phenyl]-1-*m*-tolylpropa-1,2-dienyl]trimethylsilane (19e). Column chromatography, *n*-pentane/dichloromethane (49:1), R_f = 0.51, yellow oil: 80% yield (4.65 mmol, 1.89 g); IR (KBr) $\tilde{\nu}$ 3064, 2960, 2208, 2179, 1931, 1487, 1369, 1222, 1045, 957, 845, 760 cm^{-1}; ^{1}H NMR (400 MHz, C_6D_6) δ 0.28 (s, 9H, 9-H), 2.07 (s, 3H, 14-H), 2.46 (s, 6H, 3-H), 6.86−6.90 (m, 4H, 2,5,11-H), 6.94−6.97 (m, 1H, 1-H), 7.01 (td, J = 7.8, 1.2 Hz, 1H, 6-H), 7.10 (t, J = 7.8 Hz, 1H, 12-H), 7.31 (d, J = 7.8 Hz, 1H, 13-H), 7.33 (s, 1H, 8-H), 7.38 (s, 1H, 10-H), 7.52 (dd, J = 7.8, 1.2 Hz, 1H, 4-H), 7.70 (dd, J = 7.8, 1.2 Hz, 1H, 7-H) ppm; ^{13}C NMR (100 MHz, C_6D_6) δ 0.0, 21.5, 21.6, 90.2, 92.8, 97.0, 105.3, 121.9, 123.7, 125.6, 126.2, 126.7, 127.2, 128.1, 128.3, 128.9, 129.1, 129.2, 133.2, 136.7, 136.9, 138.7, 140.6, 210.4 ppm. Anal. Calcd for $C_{29}H_{30}Si$: C, 85.66; H, 7.44. Found: C, 85.32; H 7.45.

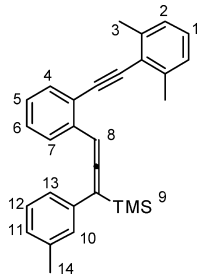

1-(Diphenylphosphinoyl)-1-(*m*-tolyl)-3-(2-phenylethynyl-phenyl)propa-1,2-diene (19f). Chlorodiphenylphosphine (452 mg, 2.05 mmol) in 5 mL of tetrahydrofuran was added to a solution of **26** (550 mg, 1.70 mmol) and NEt_3 (207 mg, 2.05 mmol) in 25 mL of tetrahydrofuran over 15 min at −78 °C. The reaction mixture was stirred for 1 h at the same temperature and then allowed to warm to 0 °C slowly. After being stirred for 1 h, the mixture was hydrolyzed with water and extracted with ethyl acetate three times. The combined organic layers were dried over magnesium sulfate and concentrated under reduced pressure. After purification by flash column chromatography using cold eluant (silica gel, *n*-hexane/ethyl acetate = 3:2, R_f = 0.25), **19f** was isolated in 46% yield (398 mg, 786 μmol) as an orange flurry solid. This thermolabile compound (T_{onset} = 53 °C) was used for thermolysis immediately: IR (KBr) $\tilde{\nu}$ 3056, 2920, 2862, 2279, 1924, 1599, 1493, 1437, 1196, 1117, 756, 694 cm^{-1}; ^{1}H NMR (400 MHz, C_6D_6) δ 1.97 (s, 3H, 13-H), 6.71−7.03 (m, 14H, Ar-H), 7.08 (d, J = 10.5 Hz, 1H, 8-H), 7.36−7.39 (m, 4H, Ar-H), 7.95−8.00 (m, 5H, 7, 14-H) ppm; ^{13}C NMR (100 MHz, C_6D_6) δ 21.3, 87.9, 95.2, 96.7 (d, J_{C-P} = 12.0 Hz), 106.9 (d, J_{C-P} = 96 Hz), 126.3 (d, J_{C-P} = 4.3 Hz), 127.8, 128.5, 128.7 (d, J_{C-P} = 4.3 Hz), 128.9, 129.1, 129.2, 129.5, 129.6, 131.7 (d, J_{C-P} = 7.1 Hz), 131.8 (d, J_{C-P} = 7.1 Hz), 131.9, 132.0 (d, J_{C-P} = 9.4 Hz), 132.1 (d, J_{C-P} = 9.4 Hz), 132.3 (d, J_{C-P} = 9.4 Hz), 132.9, 133.5 (d, J_{C-P} = 105 Hz), 134.0 (d, J_{C-P} = 105 Hz), 134.3 (d, J_{C-P} = 7.1 Hz), 138.7, 213.5 (d, J_{C-P} = 6.0 Hz) ppm. Further characterization was not possible due to the thermal lability.

dx.doi.org/10.1021/jo302524a | J. Org. Chem. 2013, 78, 1451−1462

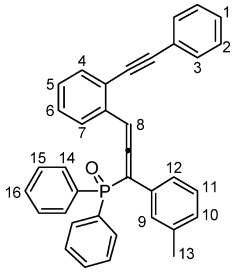

General Procedure for Thermolysis of Enyne−Allenes 19a−f Generating Cyclized Products 20a−f and 21a−f. A solution of 100 mg of enyne−allene in dry and degassed toluene was taken in a sealed tube and heated for 10−15 min at 140 °C to complete the cyclization. After removal of toluene under reduced pressure and purification by chromatography (preparative TLC, silica gel 60 F_{254}) the two constitutional isomers were purified and characterized either in mixture or in separated form.

(6-Methyl-5-phenyl-11*H*-benzo[*b*]fluoren-10-yl)diphenylphosphine Oxide (20f). Preparative TLC, *n*-pentane/ethylacetate (3:2), R_f = 0.46, white semisolid: 36% yield (71 μmol, 36.0 mg); IR (KBr) $\tilde{\nu}$ 3056, 2963, 2930, 2855, 2359, 2338, 1732, 1437, 1365, 1261, 1188, 1116, 1100, 953, 800, 759, 744, 722, 697 cm^{-1}; ^1H NMR (400 MHz, CD_2Cl_2) δ 2.05 (s, 3H, 12-H), 4.03 (s, 2H, 8-H), 5.85 (d, J = 7.6 Hz, 1H, 7-H), 6.88 (td, J = 7.6, 1.0 Hz, 1H, 6-H), 7.07 (t, J = 7.8 Hz, 1H, 10-H), 7.13 (d, J = 7.8 Hz, 1H, 11-H), 7.14 (t, J = 7.6 Hz, 1H, 5-H), 7.31 (d, J = 7.6 Hz, 1H, 4-H), 7.47−7.52 (m, 6H, 2,14-H), 7.55−7.63 (m, 5H, 1, 3, 15-H), 7.78 (ddd, J_{H-P} = 15.6 Hz, J = 8.4 Hz, J = 1.3 Hz, 4H, 13-H), 8.29 (d, J = 7.8 Hz, 1H, 9-H) ppm; ^{13}C NMR (100 MHz, CD_2Cl_2) δ 26.5, 39.2 (d, J_{C-P} = 3.1 Hz), 123.5 (d, J_{C-P} = 102 Hz), 124.3, 124.6, 125.3, 126.5, 127.2 (d, J_{C-P} = 7.3 Hz), 127.6, 128.4, 129.1 (d, J_{C-P} = 12.0 Hz), 129.3, 130.3, 131.9 (d, J_{C-P} = 8.4 Hz), 132.1, 132.2, 132.2 (d, J_{C-P} = 9.5 Hz), 134.4 (d, J_{C-P} = 9.2 Hz), 135.5 (d, J_{C-P} = 102 Hz), 137.3, 139.7 (d, J_{C-P} = 2.9 Hz), 140.0 (d, J_{C-P} = 12.4 Hz), 140.3, 142.8, 144.8, 149.3 (d, J_{C-P} = 8.3 Hz) ppm; HRMS-EI (m/z) for $C_{36}H_{27}OP$ $[M]^+$ calcd 506.180, found 506.180.

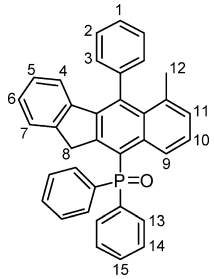

(8-Methyl-5-phenyl-11*H*-benzo[*b*]fluoren-10-yl)diphenylphosphine Oxide (21f). Preparative TLC, *n*-pentane/ethylacetate (3:2), R_f = 0.43, white semisolid: 41% yield (80.9 μmol, 41.0 mg); IR (KBr) $\tilde{\nu}$ 3058, 2922, 2852, 2360, 2341, 1733, 1620, 1589, 1510, 1437, 1394, 1329, 1184, 1117, 1101, 1071, 1028, 920, 905, 822, 768, 763, 729, 697 cm^{-1}; ^1H NMR (400 MHz, CD_2Cl_2) δ 2.18 (s, 3H, 10-H), 4.05 (d, J_{H-P} = 1.6 Hz, 2H, 8-H), 6.31 (d, J = 7.8 Hz, 1H, 7-H), 6.95 (td, J = 7.8, 0.8 Hz, 1H, 6-H), 7.13−7.18 (m, 2H, 5, 11-H), 7.33 (d, J = 7.8 Hz, 1H, 4-H), 7.40 (dd, J = 7.6, 1.8 Hz, 2H, 3-H), 7.45 (dd, J = 8.3 Hz, J_{H-P} = 1.8 Hz, 1H, 12-H), 7.50 (tdd, J = 8.0 Hz, J_{H-P} = 3.0 Hz, J = 1.2 Hz, 4H, 14-H), 7.57−7.66 (m, 5H, 1,2,15-H), 7.78 (ddd, J_{H-P} = 15.6 Hz, J = 8.0 Hz, J = 1.3 Hz, 4H, 13-H), 8.05 (d, J = 0.6 Hz, 1H, 9-H) ppm; ^{13}C NMR (100 MHz, CD_2Cl_2) δ 21.8, 39.3 (d, J_{C-P} = 2.7 Hz), 122.1 (d, J_{C-P} = 99.2 Hz), 123.7, 124.7, 126.6, 127.0 (d, J_{C-P} = 5.7 Hz), 127.2, 127.6, 127.7, 128.4, 129.1(d, J_{C-P} = 12.0 Hz), 129.6, 129.9, 131.8 (d, J_{C-P} = 8.9 Hz), 132.1 (d, J_{C-P} = 9.9 Hz), 132.2 (d, J_{C-P} = 2.8 Hz), 133.4 (d, J_{C-P} = 9.3 Hz), 135.4 (d, J_{C-P} = 101.8 Hz), 135.9, 137.6 (d, J_{C-P} = 11.9 Hz), 138.6 (d, J_{C-P} = 2.6 Hz), 139.1, 139.8, 144.7, 150.2 (d, J_{C-P} = 9.3 Hz) ppm; HRMS-EI (m/z) for $C_{36}H_{27}OP$ $[M]^+$ calcd 506.180, found 506.180.

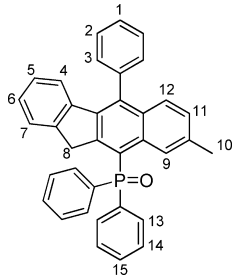

Thermolysis of Trimethyl(3-(2-(phenylethynyl)phenyl)-1-*m*-tolylpropa-1,2-dienyl)silane (19a) Yielding 20a and 21a. Preparative TLC, *n*-pentane, R_f = 0.16, yellow oil: 88% yield (232 μmol, 88.0 mg); IR (KBr) $\tilde{\nu}$ 3059, 3027, 2952, 2931, 2901, 2866, 1601, 1492, 1464, 1443, 1397, 1264, 1251, 904, 840, 762, 702 cm^{-1}; ^1H NMR (400 MHz, C_6D_6) δ 0.57 (s, 9H, 9-H), 0.60 (s, 9H, 22-H), 2.13 (s, 3H, 13-H), 2.36 (s, 3H, 24-H), 3.99 (s, 2H, 8-H), 4.02 (s, 2H, 21-H), 6.26 (d, J = 8.0 Hz, 1H, 7-H), 6.75 (d, J = 7.8 Hz, 1H, 20-H), 6.93 (td, J = 8.0, 1.0 Hz, 1H, 6-H, semicovered), 6.96 (td, J = 7.8, 1.0 Hz, 1H, 19-H, semicovered), 7.06 (td, J = 7.8, 1.0 Hz, 1H, 5-H, semicovered), 7.07−7.10 (m, 3H, 11, 18, 25-H), 7.17−7.40 (m, 13H, 1, 2, 3, 4, 12, 14, 15, 16, 17-H), 7.76 (d, J = 8.8 Hz, 1H, 26-H), 8.26 (s, 1H, 23-H), 8.37 (d, J = 8.5 Hz, 1H, 10-H) ppm; ^{13}C NMR (100 MHz, C_6D_6) δ 3.37, 3.51, 21.9, 26.8, 39.7, 39.8, 121.3, 124.1, 124.7, 124.8, 125.5, 126.7, 126.8, 127.1, 127.2 (2C), 127.9, 128.0, 128.2, 128.9 (2C), 129.5, 129.8, 130.4, 130.8 (2C), 130.9, 131.6, 131.7, 132.7, 134.4, 135.8, 136.7, 136.8, 137.2, 137.5, 138.6, 138.9, 140.2, 141.5, 141.9, 143.9, 144.5, 144.6, 147.9, 148.9 ppm; HRMS-EI (m/z) for $C_{27}H_{26}Si$ $[M]^+$ calcd 378.180, found 378.180.

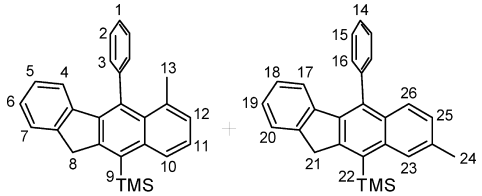

20a **21a**

Thermolysis of (3-(2-((*p*-Fluorophenyl)ethynyl)phenyl)-1-*m*-tolylpropa-1,2-dienyl)trimethylsilane (19b) Yielding 20b and 21b. Preparative TLC, *n*-pentane, R_f = 0.46, colorless oil: 85% yield (214 μmol, 85.0 mg); IR (KBr) $\tilde{\nu}$ 3044, 2953, 2900, 1603, 1512, 1464, 1252, 1222, 1157, 907, 855, 763 cm^{-1}; ^1H NMR (400 MHz, C_6D_6) δ 0.56 (s, 9H, 8-H), 0.59 (s, 9H, 20-H), 2.02 (s, 3H, 12-H), 2.37 (s, 3H, 22-H), 3.96 (s, 2H, 7-H), 3.99 (s, 2H, 19-H), 6.22 (d, J = 8.0 Hz, 1H, 6-H), 6.69 (d, J = 7.8 Hz, 1H, 18-H), 6.83 (t, J = 8.8 Hz, J_{H-F} = 8.8 Hz, 2H, 1-H), 6.91−6.96 (m, 3H, 5, 13-H), 6.98 (td, J = 7.8, 0.8 Hz, 1H, 17-H), 7.03−7.13 (m, 8H, 2, 4, 10, 14, 16, 23-H), 7.25−7.30 (m, 3H, 3, 11, 15-H), 7.62 (d, J = 8.0 Hz, 1H, 24-H), 8.26 (s, 1H, 21-H), 8.35 (d, J = 8.0 Hz, 1H, 9-H) ppm; ^{13}C NMR (100 MHz, C_6D_6) δ 3.3, 3.4, 21.9, 26.9, 39.6, 40.7, 115.6 (d, J_{C-F} = 19.3 Hz) 116.4 (d, J_{C-F} = 19.3 Hz), 123.8, 124.4, 124.7, 124.8 (2C), 124.9, 126.8, 126.9, 127.2, 127.2, 127.3, 127.5, 128.2, 129.9, 131.3, 131.6, 131.8, 132.0 (d, J_{C-F} = 7.7 Hz), 132.3 (d, J_{C-F} = 7.7 Hz), 133.0, 134.5, 134.5, 135.5, 135.8 (d, J_{C-F} = 3.4 Hz), 136.9, 136.9, 137.4, 138.5, 139.1, 139.6 (d, J_{C-F} = 3.7 Hz), 141.2, 141.6, 144.4, 144.7, 147.9, 148.8, 162.9 (d, J_{C-F} = 244.8 Hz) 163.0 (d, J_{C-F} = 245.3 Hz) ppm; HRMS-EI (m/z) for $C_{27}H_{25}FSi$ $[M]^+$ calcd 396.171, found 396.171.

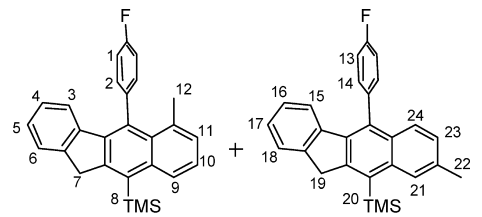

20b **21b**

Thermolysis of Trimethyl(1-*m*-tolyl-3-(2-(*p*-tolylethynyl)-phenyl)propa-1,2-dienyl)silane (19c) Yielding 20c and 21c. Preparative TLC, *n*-pentane, R_f = 0.57, yellow oil: 76% yield (194

dx.doi.org/10.1021/jo302524a | J. Org. Chem. 2013, 78, 1451−1462

μmol, 76.0 mg); IR (KBr) $\tilde{\nu}$ 3058, 2958, 2155, 1930, 1758, 1598, 1483, 1445, 1249, 843, 758 cm^{-1}; ^1H NMR (400 MHz, C_6D_6) δ 0.57 (s, 9H, 9-H), 0.60 (s, 9H, 22-H), 2.19 (s, 6H, 1, 14-H), 2.23 (s, 3H, 13-H), 2.36 (s, 3H, 24-H), 4.00 (s, 2H, 8-H), 4.02 (s, 2H, 21-H), 6.42 (d, J = 8.0 Hz, 1H, 7-H), 6.90 (d, J = 8.0 Hz, 1H, 20-H), 6.99−7.00 (m, 2H, 11, 17-H), 7.03−7.06 (m, 4H, 3, 16-H), 7.07−7.17 (m, 3H, 4, 6, 12-H), 7.26−7.34 (m, 8H, 2, 5, 15, 18, 19, 25-H), 7.83 (d, J = 8.0 Hz, 1H, 26-H), 8.26 (s, 1H, 23-H), 8.37 (d, J = 8.0 Hz, 1H, 10-H) ppm; ^{13}C NMR (100 MHz, C_6D_6) δ 3.4, 3.5, 21.4, 21.9, 26.9 (2C), 39.7, 39.8, 124.1, 124.6, 124.7, 124.8, 124.8, 126.7, 126.8, 127.1, 127.1, 127.9, 128.1, 129.7 (2C), 129.8, 130.2 (2C), 130.6 (2C), 130.8, 131.9, 132.0, 132.6, 134.3, 135.9, 136.8, 136.8, 137.2, 137.3, 137.3, 137.4, 137.5, 138.6, 139.1, 140.8, 141.6, 142.0, 144.4, 144.6, 148.0, 148.9 ppm; HRMS-EI (m/z) for $C_{28}H_{28}Si$ $[M]^+$ calcd 392.196, found 392.196.

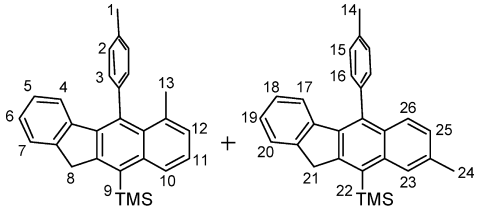

20c **21c**

Thermolysis of [3-[2-(*p*-Anisylethynyl)phenyl]-1-*m*-tolylpropa-1,2-dienyl]trimethylsilane (19d) Yielding 20d and 21d. Preparative TLC, *n*-pentane, R_f = 0.31, yellow oil: 47% yield (115 μmol, 47.0 mg); IR (KBr) $\tilde{\nu}$ 3424, 2954, 2280, 1609, 1515, 1283, 1245, 1034, 906, 852, 763 cm^{-1}; ^1H NMR (400 MHz, C_6D_6) δ 0.58 (s, 9H, 9-H), 0.61 (s, 9H, 22-H), 2.19 (s, 3H, 13-H), 2.38 (s, 3H, 24-H), 3.34 (s, 3H, 1-H), 3.38 (s, 3H, 14-H), 3.99 (s, 2H, 8-H), 4.01 (s, 2H, 21-H), 6.47 (d, J = 7.8 Hz, 1H, 7-H), 6.83 (d, J = 8.6 Hz, 2H, 2-H), 6.90−7.01 (m, 5H, 6, 15, 19, 20-H), 7.07 (td, J = 7.8, 1.0 Hz, 1H, 5-H, semicovered), 7.09 (td, J = 7.8, 1.0 Hz, 1H, 18-H, semicovered), 7.11−7.13 (m, 2H, 12, 25-H), 7.21 (d, J = 8.6 Hz, 2H, 3-H), 7.27−7.32 (m, 5H, 4, 11, 16, 17-H), 7.85 (d, J = 8.0 Hz, 1H, 26-H), 8.27 (s, 1H, 23-H), 8.37 (d, J = 8.0 Hz, 1H, 10-H) ppm; ^{13}C NMR (100 MHz, C_6D_6) δ 3.4, 3.5, 22.0, 26.9, 39.7, 39.8, 54.7, 54.8, 114.3, 115.0, 124.1, 124.6, 124.7, 124.7, 124.8, 126.8, 126.9, 127.1 (2C), 127.9, 128.1, 129.8 (2C), 130.8, 131.4, 131.7, 132.1, 132.2, 132.3, 132.6, 134.3, 135.7, 135.8, 136.6 (2C), 137.1, 137.3, 137.5, 138.6, 139.5, 141.6, 142.1, 144.4, 144.6, 148.0, 148.9, 159.7, 159.8 ppm. Anal. Calcd for $C_{28}H_{28}OSi$: C, 82.30; H, 6.91. Found: C, 82.48; H, 7.15.

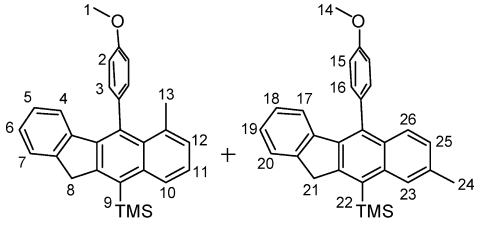

20d **21d**

Thermolysis of [3-[2-(2,6-Dimethylphenylethynyl)phenyl]-1-*m*-tolylpropa-1,2-dienyl]trimethylsilane (19e) Yielding 20e and 21e. Preparative TLC, *n*-pentane, R_f = 0.45, yellow oil: 34% yield (83.6 μmol, 34.0 mg); IR (KBr) $\tilde{\nu}$ 3062, 2951, 2930, 2855, 2361, 2342, 2279, 1464, 1251, 904, 870, 840, 764 cm^{-1}; ^1H NMR (400 MHz, C_6D_6) δ 0.55 (s, 9H, 9-H), 0.58 (s, 9H, 22-H), 1.90 (s, 6H, 3-H), 1.92 (s, 6H, 16-H), 2.15 (s, 3H, 13-H), 2.36 (s, 3H, 24-H), 4.03 (s, 2H, 8-H), 4.05 (s, 2H, 21-H), 6.36 (d, J = 8.0 Hz, 1H, 7-H), 6.77 (d, J = 7.8 Hz, 1H, 20-H), 6.97 (t, J = 8.0 Hz, 1H, 6-H, semicovered), 6.99 (t, J = 7.8 Hz, 1H, 19-H, semicovered), 7.06 (d, J = 8.0 Hz, 2H, 2-H, semicovered), 7.07−7.11 (m, 3H, 5, 18, 25-H), 7.11 (d, J = 8.0 Hz, 1H, 12-H, semicovered), 7.18 (d, J = 8.0 Hz, 2H, 15-H), 7.26−7.32 (m, 5H, 1, 4, 11, 14, 17-H), 7.66 (d, J = 7.8 Hz, 1H, 26-H), 8.28 (s, 1H, 23-H), 8.38 (d, J = 8.0 Hz, 1H, 10-H) ppm; ^{13}C NMR (100 MHz, C_6D_6) δ 3.4, 3.5, 20.1, 20.5, 21.9, 25.0, 39.8, 39.9, 122.7, 123.4. 124.7 (2C), 124.8, 126.5, 127.3, 127.4, 127.4, 127.5, 127.6, 127.9, 128.1, 128.4, 128.4, 128.8, 128.6, 129.7, 130.4, 130.8, 131.1, 132.5, 132.6, 134.2, 134.7, 135.2, 136.4, 136.9, 137.3, 137.8, 137.9, 138.6, 140.0, 141.5, 141.7, 142.6, 144.4, 144.6, 148.6, 149.3 ppm. Anal. Calcd for $C_{29}H_{30}Si$: C, 85.66; H, 7.44. Found: C, 85.36; H, 7.66.

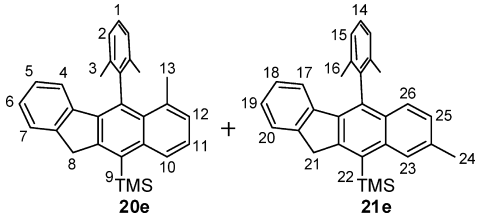

20e **21e**

■ ASSOCIATED CONTENT

Supporting Information

^1H and ^{13}C NMR spectra of all relevant compounds and computational data. This material is available free of charge via the Internet at http://pubs.acs.org.

■ AUTHOR INFORMATION

Corresponding Author

*E-mail: schmittel@chemie.uni-siegen.de.

Notes

The authors declare no competing financial interest.

■ ACKNOWLEDGMENTS

We are indebted to the Deutsche Forschungsgemeinschaft and University of Siegen for continued support of our research.

■ REFERENCES

(1) Steinfeld, J. I.; Francisco, J. S.; Hase, W. L. *Chemical Kinetics and Dynamics*, 2nd ed.; Prentice Hall: Upper Saddle River, NJ, 1998.

(2) (a) Gilbert, R. G.; Smith, S. C. *Theory of Unimolecular and Recombination Reactions*; Blackwell Scientific: Oxford, 1990. (b) Baer, T.; Hase, W. L. *Unimolecular Reaction Dynamics. Theory and Experiment*; Oxford University Press: New York, 1996.

(3) (a) Sun, L.; Song, K.; Hase, W. L. *Science* **2002**, *296*, 875. (b) Mikosch, J.; Otto, R.; Trippel, S.; Eichhorn, C.; Weidemüller, M.; Wester, R. *J. Phys. Chem. A* **2008**, *112*, 10448. (c) Bogle, X. S.; Singleton, D. A. *Org. Lett.* **2012**, *14*, 2528.

(4) (a) Schmittel, M.; Vavilala, C.; Jaquet, R. *Angew. Chem., Int. Ed.* **2007**, *46*, 6911. (b) Glowacki, D. R.; Marsden, S. P.; Pilling, M. J. *J. Am. Chem. Soc.* **2009**, *131*, 13896. (c) Lan, Y.; Danheiser, R. L.; Houk, K. N. *J. Org. Chem.* **2012**, *77*, 1533.

(5) (a) Nummela, J. A.; Carpenter, B. K. *J. Am. Chem. Soc.* **2002**, *124*, 8512. (b) Zhou, J.; Schlegel, H. B. *J. Phys. Chem. A* **2008**, *112*, 13121. (c) Zhou, J.; Schlegel, H. B. *J. Phys. Chem. A* **2009**, *113*, 1453. (d) Zhou, J.; Schlegel, H. B. *Theor. Chem. Acc.* **2012**, *131*, 1126.

(6) (a) Bach, A.; Hostettler, J. M.; Chen, P. *J. Chem. Phys.* **2006**, *125*, 024304. (b) Gasser, M.; Frey, J. A.; Hostettler, J. M.; Bach, A. *Chem. Commun.* **2011**, *47*, 301.

(7) (a) Ammal, S. C.; Yamataka, H.; Aida, M.; Dupuis, M. *Science* **2003**, *299*, 1555. (b) Ussing, B. R.; Singleton, D. A. *J. Am. Chem. Soc.* **2005**, *127*, 2888.

(8) (a) Carpenter, B. K. *Acc. Chem. Res.* **1992**, *25*, 520. (b) Carpenter, B. K. *Angew. Chem.* **1998**, *110*, 3532. (c) Carpenter, B. K. *Chem. Soc. Rev.* **2006**, *35*, 736.

(9) (a) Kless, A.; Nendel, M.; Wilsey, S.; Houk, K. N. *J. Am. Chem. Soc.* **1999**, *121*, 4524. (b) Wang, Z.; Hirschi, J. S.; Singleton, D. A. *Angew. Chem., Int. Ed.* **2009**, *48*, 9156. (c) Xu, L.; Doubleday, C. E.; Houk, K. N. *J. Am. Chem. Soc.* **2010**, *132*, 3029. (d) Alder, R. W.; Harvey, J. N.; Lloyd-Jones, G. C.; Oliva, J. M. *J. Am. Chem. Soc.* **2010**, *132*, 8325. (e) Herath, N.; Suits, A. G. *J. Phys. Chem. Lett.* **2011**, *2*, 642. (f) Gonzalez-James, O. M.; Kwan, E. E.; Singleton, D. A. *J. Am. Chem. Soc.* **2012**, *134*, 1914.

(10) (a) Jones, R. R.; Bergman, R. G. *J. Am. Chem. Soc.* **1972**, *94*, 660. (b) Bergman, R. G. *Acc. Chem. Res.* **1973**, *6*, 25.

(11) (a) Myers, A. G.; Kuo, E. Y.; Finney, N. S. *J. Am. Chem. Soc.* **1989**, *111*, 8057. (b) Nagata, R.; Yamanaka, H.; Okazaki, E.; Saito, I. *Tetrahedron Lett.* **1989**, *30*, 4995.
(12) (a) Wang, K. K. *Chem. Rev.* **1996**, *96*, 207. (b) Basak, A.; Mandal, S.; Bag, S. S. *Chem. Rev.* **2003**, *103*, 4077. (c) Wenk, H. H.; Winkler, M.; Sander, W. *Angew. Chem., Int. Ed.* **2003**, *42*, 502. (d) Kar, M.; Basak, A. *Chem. Rev.* **2007**, *107*, 2861.
(13) (a) Norizuki, Y.; Komano, K.; Sato, I.; Hirama, M. *Chem. Commun.* **2008**, 5372. (b) Pandithavidana, D. R.; Poloukhtine, A.; Popik, V. V. *J. Am. Chem. Soc.* **2009**, *131*, 351. (c) Vinogradova, O. V.; Balova, I. A.; Popik, V. V. *J. Org. Chem.* **2011**, *76*, 6937. (d) Roy, S.; Anoop, A.; Biradha, K.; Basak, A. *Angew. Chem., Int. Ed.* **2011**, *50*, 8316. (e) Dong, H.; Chen, B.-Z.; Huang, M.-B.; Lindh, R. *J. Comput. Chem.* **2012**, *33*, 537. (f) Campolo, D.; Gaudel-Siri, A.; Mondal, S.; Siri, D.; Besson, E.; Vanthuyne, N.; Nechab, M.; Bertrand, M. P. *J. Org. Chem.* **2012**, *77*, 2773.
(14) (a) Nicolaou, K. C.; Dai, W.-M. *Angew. Chem., Int. Ed.* **1991**, *30*, 1387. (b) Borders, D. B.; Doyle, T. W. *Enediyne Antibiotics as Antitumor Agents*; Marcel Dekker: New York, 1995.
(15) Schmittel, M.; Strittmatter, M.; Kiau, S. *Tetrahedron Lett.* **1995**, *36*, 4975.
(16) Schmittel, M.; Vavilala, C.; Cinar, M. E. *J. Phys. Org. Chem.* **2012**, *25*, 182.
(17) (a) Schmittel, M.; Strittmatter, M.; Kiau, S. *Angew. Chem., Int. Ed.* **1996**, *35*, 1843. (b) Schmittel, M.; Strittmatter, M.; Vollmann, K.; Kiau, S. *Tetrahedron Lett.* **1996**, *37*, 999. (c) Schmittel, M.; Steffen, J.-P.; Auer, D.; Maywald, M. *Tetrahedron Lett.* **1997**, *38*, 6177. (d) Schmittel, M.; Keller, M.; Kiau, S.; Strittmatter, M. *Chem.—Eur. J.* **1997**, *3*, 807. (e) Engels, B.; Lennartz, C.; Hanrath, M.; Schmittel, M.; Strittmatter, M. *Angew. Chem., Int. Ed.* **1998**, *37*, 1960. (f) Schmittel, M.; Strittmatter, M. *Tetrahedron* **1998**, *54*, 13751. (g) Li, H.; Zhang, H.-R.; Petersen, J. L.; Wang, K. K. *J. Org. Chem.* **2001**, *66*, 6662. (h) Schmittel, M.; Steffen, J.-P.; Maywald, M.; Engels, B.; Helten, H.; Musch, P. *J. Chem. Soc., Perkin Trans. 2* **2001**, 1331. (i) Yang, Y.; Petersen, J. L.; Wang, K. K. *J. Org. Chem.* **2003**, *68*, 5832. (j) Yang, Y.; Petersen, J. L.; Wang, K. K. *J. Org. Chem.* **2003**, *68*, 8545.
(18) (a) Engels, B.; Hanrath, M. *J. Am. Chem. Soc.* **1998**, *120*, 6356. (b) Schreiner, P. R.; Prall, M. *J. Am. Chem. Soc.* **1999**, *121*, 8615. (c) Cramer, C. J.; Kormos, B. L.; Seierstad, M.; Sherer, E. C.; Winget, P. *Org. Lett.* **2001**, *3*, 1881. (d) de Visser, S. P.; Filatov, M.; Shaik, S. *Phys. Chem. Chem. Phys.* **2001**, *3*, 1242. (e) Stahl, F.; Moran, D.; von Ragué Schleyer, P.; Prall, M.; Schreiner, P. R. *J. Org. Chem.* **2002**, *67*, 1453. (f) Schreiner, P. R.; Navarro-Vazquez, A.; Prall, M. *Acc. Chem. Res.* **2005**, *38*, 29.
(19) (a) Zhang, H.-R.; Wang, K. K. *J. Org. Chem.* **1999**, *64*, 7996. (b) Wang, K. K.; Zhang, H.-R.; Petersen, J. L. *J. Org. Chem.* **1999**, *64*, 1650. (c) Dai, W.; Petersen, J. L.; Wang, K. K. *Org. Lett.* **2006**, *8*, 4665. (d) Zhang, Y.; Petersen, J. L.; Wang, K. K. *Org. Lett.* **2007**, *9*, 1025.
(20) (a) Schmittel, M.; Kiau, S.; Siebert, T.; Strittmatter, M. *Tetrahedron Lett.* **1996**, *37*, 7691. (b) Schmittel, M.; Maywald, M.; Strittmatter, M. *Synlett* **1997**, 165.
(21) Schmittel, M.; Mahajan, A. A.; Bucher, G.; Bats, J. W. *J. Org. Chem.* **2007**, *72*, 2166.
(22) Garcia, J. G.; Ramos, B.; Pratt, L. M.; Rodríguez, A. *Tetrahedron Lett.* **1995**, *36*, 7391.
(23) (a) Gillmann, T.; Hülsen, T.; Massa, W.; Wocadlo, S. *Synlett* **1995**, 1257. (b) Cinar, M. E.; Vavilala, C.; Fan, J.; Schmittel, M. *Org. Biomol. Chem.* **2011**, *9*, 3776.
(24) Vavilala, C.; Bats, J. W.; Schmittel, M. *Synthesis* **2010**, 2213.
(25) Schmittel, M.; Vavilala, C. *J. Org. Chem.* **2005**, *70*, 4865.
(26) Musch, P. W.; Engels, B. *J. Am. Chem. Soc.* **2001**, *123*, 5557.
(27) Bekele, T.; Christian, C. F.; Lipton, M. A.; Singleton, D. A. *J. Am. Chem. Soc.* **2005**, *127*, 9216.
(28) Ess, D. H.; Wheeler, S. E.; Iafe, R. G.; Xu, L.; Çelebi-Ölçüm, N.; Houk, K. N. *Angew. Chem., Int. Ed.* **2008**, *47*, 7592.
(29) (a) Carpenter, B. K. *Angew. Chem., Int. Ed.* **1998**, *37*, 3340. (b) Carpenter, B. K. *J. Phys. Org. Chem.* **2003**, *16*, 858. (c) Carpenter, B. K. In *Reactive Intermediate Chemistry*; Moss, R. A., Platz, M. S., Jones, M., Jr., Eds.; Wiley & Sons: Upper Saddle River, NJ, 2009.
(30) Chen, H.-T.; Chen, H.-L.; Ho, J.-J. *J. Phys. Org. Chem.* **2010**, *23*, 134.
(31) Larock, R. C.; Doty, M. J.; Cacchi, S. *J. Org. Chem.* **1993**, *58*, 4579.
(32) (a) Schmittel, M.; Strittmatter, M.; Schenk, W. A.; Hagel, M. *Z. Naturforsch.* **1998**, *53b*, 1015. (b) Vavilala, C. Dissertation, University of Siegen, 2007. (c) Sakamoto, T.; Kondo, Y.; Miura, N.; Hayashi, K.; Yamanaka, H. *Heterocycles* **1986**, *24*, 2311. (d) Roesch, K. R.; Larock, R. C. *J. Org. Chem.* **2002**, *67*, 86.
(33) (a) Atienza, C.; Mateo, C.; de Frutos, Ó.; Echavarren, A. M. *Org. Lett.* **2001**, *3*, 153. (b) González-Cantalapiedra, E.; de Frutos, Ó.; Atienza, C.; Mateo, C.; Echavarren, A. M. *Eur. J. Org. Chem.* **2006**, 1430.
(34) Fleming, I.; Terrett, N. K. *J. Organomet. Chem.* **1984**, *264*, 99.
(35) Elsevier, C. J.; Stehouwer, P. M.; Westmijze, H.; Vermeer, P. *J. Org. Chem.* **1983**, *48*, 1103.
(36) Carpenter, B. K. *J. Am. Chem. Soc.* **1985**, *107*, 5730.
(37) Prall, M.; Wittkopp, A.; Schreiner, P. R. *J. Phys. Chem. A* **2001**, *105*, 9265.
(38) (a) Becke, A. D. *Phys. Rev. A* **1988**, *38*, 3098. (b) Lee, C.; Yang, W.; Parr, R. G. *Phys. Rev. B* **1988**, *37*, 785.
(39) (a) Ditchfield, R.; Hehre, W. J.; Pople, J. A. *J. Chem. Phys.* **1971**, *54*, 724. (b) Hehre, W. J.; Ditchfield, R.; Pople, J. A. *J. Chem. Phys.* **1972**, *56*, 2257. (c) Hariharan, P. C.; Pople, J. A. *Theor. Chim. Acta* **1973**, *28*, 213.
(40) Frisch, M. J. et al. *Gaussian 03*, Gaussian, Inc., Wallingford, CT, 2004.
(41) Wenthold, P. G.; Lipton, M. A. *J. Am. Chem. Soc.* **2000**, *122*, 9265.
(42) Yamaguchi, K.; Jensen, F.; Dorigo, A.; Houk, K. N. *Chem. Phys. Lett.* **1988**, *149*, 537.
(43) (a) Doubleday, C.; Nendel, M.; Houk, K. N.; Thweatt, D.; Page, M. *J. Am. Chem. Soc.* **1999**, *121*, 4720. (b) Doubleday, C.; Suhrada, C. P.; Houk, K. N. *J. Am. Chem. Soc.* **2006**, *128*, 90.
(44) One of the two phenyl groups of the $POPh_2$ unit creates a rotational barrier for the probed *m*-tolyl ring in the two intermediates, **19fb** and **19fb1**, which is not present in the diradical intermediates generated from **19a-c**.
(45) Leach, A. G.; Houk, K. N. *Org. Biomol. Chem.* **2003**, *1*, 1389.
(46) Alfonsi, M.; Dell'Acqua, M.; Facoetti, D.; Arcadi, A.; Abbiati, G.; Rossi, E. *Eur. J. Org. Chem.* **2009**, 2852.
(47) Tsukamoto, H.; Ueno, T.; Kondo, Y. *Org. Lett.* **2007**, *9*, 3033.
(48) Kawano, T.; Suehiro, M.; Ueda, I. *Chem. Lett.* **2006**, *35*, 58.